



Research Paper

Melatonin improves brain function in a model of chronic Gulf War Illness with modulation of oxidative stress, NLRP3 inflammasomes, and BDNF-ERK-CREB pathway in the hippocampus

Leelavathi N. Madhu, Maheedhar Kodali, Sahithi Attaluri, Bing Shuai, Laila Melissari, Xiaolan Rao, Ashok K. Shetty*

Institute for Regenerative Medicine, Department of Molecular and Cellular Medicine, Texas A&M University College of Medicine, College Station, TX, USA



ARTICLE INFO

Keywords:

Brain-derived neurotrophic factor
cAMP response element-binding protein
Cognitive and mood function
Inflammasomes
Mitochondria
Neuroinflammation
Neurogenesis
Oxidative stress

ABSTRACT

Persistent cognitive and mood dysfunction is the primary CNS symptom in veterans afflicted with Gulf War Illness (GWI). This study investigated the efficacy of melatonin (MEL) for improving cognitive and mood function with antioxidant, antiinflammatory, and pro-cognitive effects in a rat model of chronic GWI. Six months after exposure to GWI-related chemicals and stress, rats were treated with vehicle or MEL (5, 10, 20, 40, and 80 mg/kg) for eight weeks. Behavioral tests revealed cognitive and mood dysfunction in GWI rats receiving vehicle, which were associated with elevated oxidative stress, reduced NRF2, catalase and mitochondrial complex proteins, astrocyte hypertrophy, activated microglia with NLRP3 inflammasomes, elevated proinflammatory cytokines, waned neurogenesis, and synapse loss in the hippocampus. MEL at 10 mg/kg alleviated simple and associative recognition memory dysfunction and anhedonia, along with reduced oxidative stress, enhanced glutathione and complex III, and reduced NLRP3 inflammasomes, IL-18, TNF- α , and IFN- γ . MEL at 20 mg/kg also normalized NRF2 and catalase and increased microglial ramification. MEL at 40 mg/kg, in addition, reduced astrocyte hypertrophy, activated microglia, NF- κ B-NLRP3-caspase-1 signaling, IL-1 β , MCP-1, and MIP-1 α . Moreover, MEL at 80 mg/kg activated the BDNF-ERK-CREB signaling pathway, enhanced neurogenesis and diminished synapse loss in the hippocampus, and improved a more complex hippocampus-dependent cognitive function. Thus, MEL therapy is efficacious for improving cognitive and mood function in a rat model of chronic GWI, and MEL's effect was dose-dependent. The study provides the first evidence of MEL's promise for alleviating neuroinflammation and cognitive and mood impairments in veterans with chronic GWI.

1. Introduction

Gulf War illness (GWI), observed in over a third of veterans who served in the first GW, is a chronic multisymptom illness with persistent cognitive and mood impairments identified as one of the predominant central nervous system-related problems [1–6]. The cause of GWI has been attributed to multiple factors during the GW. These include the intake of the nerve gas prophylactic drug pyridostigmine bromide (PB), the use of mosquito repellent N,N-Diethyl-*meta*-toluamide (DEET) on the skin and the insecticide permethrin (PER) on uniforms, a variety of pesticides sprayed around tents, and the interaction of various chemicals with the war-related stress [4,7–10]. The other suggested causes of GWI include possible exposures to sarin, combustion products, fuels from

burning oil wells, mustard gas, vaccines, and depleted uranium [11]. Indeed, studies by multiple research groups have demonstrated that exposure to low to moderate doses of GWI-related chemicals (alone or in combinations) with or without stress in rodents results in persistent cognitive and mood impairments [12–22].

Studies in both animal models and veterans have suggested that cognitive and mood impairments in GWI are associated with increased oxidative stress and/or neuroinflammation in the brain. Elevated oxidative stress in animal models of chronic GWI is exemplified by higher levels of malondialdehyde (MDA), protein carbonyls (PCs), and increased expression of genes encoding proteins linked to the regulation of oxidative stress, antioxidant activity, and mitochondrial respiration [20,22,23]. Neuroinflammation in rodent models of GWI comprise

* Corresponding author. Institute for Regenerative Medicine, Texas A&M Health Science Center, College of Medicine, 1114 TAMU, 206 Olsen Boulevard College Station, TX, 77843, USA.

E-mail address: akskrs@tamu.edu (A.K. Shetty).

<https://doi.org/10.1016/j.redox.2021.101973>

Received 19 January 2021; Received in revised form 5 April 2021; Accepted 9 April 2021

Available online 22 April 2021

2213-2317/Published by Elsevier B.V. This is an open access article under the CC BY-NC-ND license (<http://creativecommons.org/licenses/by-nc-nd/4.0/>).

astrocyte hypertrophy, the transformation of a significant percentage of microglia into a persistent proinflammatory state, leakage of high mobility group box 1 protein (HMGB1) into the extracellular space, increased concentration of multiple proinflammatory cytokines, and complement C3 [16,20–25]. Consistent with this, a positron emission tomography study using [^{11}C]PBR28 suggested the occurrence of activated microglia and reactive astrocytes in the brain of veterans with GWI [26]. Studies in animal models of GWI have also suggested additional changes in the brain, which include the reduced proliferation of neural stem cells leading to a substantially reduced adult hippocampal neurogenesis [22] and adverse alterations in lipid metabolism, cellular bioenergetics, peroxisomes, lysosomes, and mitochondria [27,28]. Furthermore, the contribution of systemic inflammation to persistent cognitive and mood dysfunction has been suggested. The systemic changes include: (i) elevated levels of oxidative stress markers and proinflammatory cytokines and chemokines in the circulating blood [22, 23]; the activation of the peripheral adaptive immune response via a metabolite of PER [29]; and microbiome alterations in the gut inducing portal endotoxemia and toll-like receptor 4 (TLR4) activation [30,31]. Leakage of HMGB1 into the extracellular space in the brain [21] and elevated levels of HMGB1 in the circulating blood [32] in GWI could enhance the formation of nucleotide-binding oligomerization domain Leucine rich Repeat and Pyrin domain containing 3 (NLRP3) inflammasomes. Increased inflammasomes could interfere with the brain-derived neurotrophic factor (BDNF) and contribute to cognitive dysfunction [32]. Thus, it is likely that both incessantly elevated oxidative stress and chronic neuroinflammation underlie persistent cognitive and mood dysfunction in GWI. Therefore, drugs having robust antioxidant and antiinflammatory properties with no adverse side effects have received significant attention for treating GWI [20,22].

In this study, we investigated the efficacy of melatonin (MEL) for improving cognitive and mood function in a rat model of chronic GWI. MEL, an endogenous neurohormone derived from tryptophan, is widely used as a dietary supplement [33,34]. We chose MEL for treating chronic GWI because of its ability to reduce the toxicity of ROS [35], diminish microglial activation [36], and activate the BDNF, the extracellular signal-regulated kinase, and cAMP response element-binding protein (BDNF-ERK-CREB) signaling pathway to improve cognitive function [37]. Furthermore, MEL could also modulate NF- κ B activation, conserve mitochondrial homeostasis, and blunt the NF- κ B-NLRP3-Caspase-1 signaling in inflammatory conditions [38–40]. The rats with chronic GWI (i.e., 6-months after exposure to GWI-related chemicals and stress) were treated with vehicle or MEL (5, 10, 20, 40, and 80 mg/kg) for eight weeks. A battery of behavioral tests conducted after the treatment regimen revealed dose-dependent efficacy of MEL for improving cognitive and mood function in GWI rats, with lower (10–20 mg/kg) doses improving several cognitive tasks and mood function with the

suppression of oxidative stress and NLRP3 inflammasomes. Furthermore, moderate MEL doses (40–80 mg/kg) mediated robust anti-inflammatory activity with modulation of NF- κ B-NLRP3-caspase-1 pathway, and 80 mg/kg MEL activated the BDNF-ERK-CREB pathway and improved a more complex cognitive function.

2. Materials and methods

2.1. Animals

Eight-week-old male Sprague Dawley rats ($n = 112$; Harlan, Indianapolis, IN) housed with *ad libitum* access to food (4% fat diet; Envigo, Indianapolis, IN) and water were randomly assigned to either the naïve control group ($n = 16$) or the GWI group ($n = 96$). The institutional animal care and use committee of the Texas A&M University approved all studies conducted in this investigation. Fig. 1 illustrates the overview of the experimental design and timelines of different experiments performed in the study.

2.2. GWIR-chemicals and restraint stress exposure regimen

The animals in the GWI group ($n = 96$) received daily doses of PB orally, DEET and PER dermally, and 15-min restraint stress for four weeks, as described in our previous studies [20–23]. The doses comprised 2 mg/kg PB (Sigma, St. Louis, MO) in 0.5 ml of sterile water, 60 mg/kg DEET (Chem Service Inc, West Chester, PA) in 0.2 ml of 70% ethanol, and 0.2 mg/kg PER (Chem Service Inc) in 0.2 ml of 70% ethanol. The chemicals DEET and PER were applied sequentially on the skin over the dorsal surface of the neck and the area between scapulae. Age-matched naïve control animals ($n = 16$) maintained parallel to GWI animals, were not subjected to the chemical or stress exposure.

2.3. Treatment of GWI animals with MEL

After a survival period of six months, animals exposed to GWIR-chemicals and stress (i.e., GWI-rats) were randomly assigned to the vehicle group (GWI-Veh group, $n = 16$) or one of the five groups receiving 5, 10, 20, 40, or 80 mg/kg MEL (GWI-MEL5; GWI-MEL10; GWI-MEL20; GWI-MEL40; GWI-MEL80 groups, $n = 15$ –16/group). One animal each from GWI-MEL10 and GWI-MEL40 died during the survival period. MEL, purchased from Sigma Aldrich (St. Louis, MO) and dissolved in 0.5 ml of sterile water, was administered orally for eight weeks (5 days/week). Animals in the GWI-Veh group received 0.5 ml of sterile water for a similar duration (5 days/week). After completing the MEL or Veh treatment regimen, animals were interrogated with a series of behavioral tests.

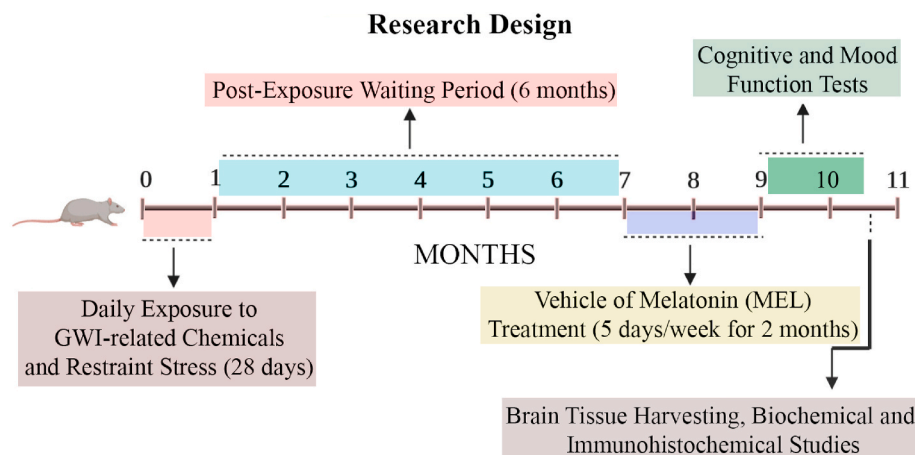


Fig. 1. The figure depicts an overview of the experimental design. The figure shows MEL treatment timelines to rats with Gulf War Illness (GWI), neuro-behavioral studies, and brain tissue analyses. The rats were first exposed to GWI-related chemicals pyridostigmine bromide, DEET, and permethrin, and 15 min of restraint stress for 28 days. Six months later, GWI rats received vehicle or MEL (5, 10, 20, 40, and 80 mg/kg, five days/week) for two months. In the next two months, animals were next interrogated with a battery of behavioral tests to ascertain cognitive and mood function, and brain tissues were harvested for biochemical assays and immunohistochemical studies.

2.4. Evaluation of the hippocampus-dependent cognitive function

The proficiency of animals to recognize subtle alterations in their proximate environment was evaluated by a hippocampus-dependent object location test (OLT), as detailed in our previous report [22]. Briefly, each animal was subjected to three successive trials (T1-T3). The first two trials comprised a habituation phase (T1) in which the animal explored the empty open field box for 5 min and a sample phase (T2) where the animal explored two similar objects placed on the right and left sides of the open field apparatus for 5 min. Sixty minutes later, in T3, the animal was allowed to explore the same two objects with one object placed in its original place (object in the familiar place), and the other object moved to another location (object in a novel place) for 5 min. The behavior of each rat in T2 and T3 was video-recorded and analyzed using AnyMaze software. A predilection for exploring the object in the novel place reflects the animal's competence to discern minor changes in objects' location in its immediate environment. Times spent with objects in the novel and familiar locations in T3, and the total object exploration times in T2 and T3 were obtained. The percentages of exploration times spent with the object in the novel place versus the object in the familiar place were statistically analyzed in each group.

2.5. Assessment of the recognition memory function

A recognition memory task, reliant on the perirhinal cortex and the hippocampus's function, was appraised in each animal using a novel object recognition test (NORT), as described in our prior reports [17]. In the first two trials, each animal successively explored an empty open field box for 5 min (T1), and two similar objects placed diagonally on the right and left sides of the open field apparatus for 5 min (T2). Thirty minutes later, in T3, the animal was allowed to explore one of the objects from T2 (i.e., the familiar object) and a new object (i.e., the novel object). The behavior of each rat in T2 and T3 was video-recorded and analyzed using AnyMaze software. A preference to explore a novel object over the familiar object in this task indicates the animal's aptitude for making recognition memory. Times spent with the familiar and novel objects, and the total object exploration times in T2 and T3 were obtained. The percentages of exploration times spent with the novel object vis-à-vis the familiar object were statistically analyzed in each group.

2.6. Appraisal of associative recognition memory function

An associative recognition memory task, dependent on an interaction between the hippocampus, the perirhinal cortex, and the medial prefrontal cortex [41], was evaluated in each animal using an object-in-place test (OIPT). The test allows investigation of an animal's ability to make an association between an object and the place in which the object was previously encountered. In the first two trials, each animal sequentially explored an empty open field box for 5 min (T1), and four different objects placed in four quadrants of the open field apparatus for 5 min (T2). Thirty minutes later, in T3, the animal was allowed to explore the same four objects, with two objects from T2 remaining in their original locations and the other two objects from T2 changing their locations through a diagonal swapping. The behavior of each rat in T2 and T3 was video-tracked using the Any-maze video-tracking system. The results, such as times spent with objects located in familiar or new locations (for swapped objects) and the total object exploration times for T2 and T3, were collected. The percentages of exploration times spent with objects positioned in familiar locales versus objects placed in novel locations were statistically evaluated in each group.

2.7. Evaluation of anhedonia

A sucrose preference test (SPT) was employed to investigate anhedonia in rats belonging to different groups. Anhedonia, a condition in which the ability to feel pleasure in activities that typically bring joy is

lost, serves as a measure of depressive-like behavior [42]. The test comprised four days of monitoring. The animals were housed individually and given 24-h access to two identical bottles containing 1% sucrose solution. One bottle was replaced with a new bottle containing regular water for 24 h on day 2. On day 3, the animals were deprived of water and food for 22 h. Each animal was then given access to two bottles, one containing 100 ml of sucrose solution and another containing 100 ml of regular water. Two hours later, the sucrose and water bottles' fluid consumption was recorded and statistically evaluated in each group.

2.8. Euthanasia and harvesting of brain tissues

The fixed brain tissues for histological studies ($n = 7-8/\text{group}$) and fresh brain tissues for biochemical and molecular biological studies ($n = 7-8/\text{group}$) were harvested, as detailed in our previous reports [20-23, 43,44]. The fresh brain tissues were snap-frozen in liquid nitrogen and stored at -80°C .

2.9. Preparation of lysate from the hippocampal tissue

The hippocampus micro-dissected from the harvested unfixed brains was lysed individually through sonication in a tissue extraction reagent (Invitrogen, Waltham, MA) containing protease inhibitor (Sigma Aldrich, 1:100 dilution) for 15-20 s at 4°C . The resulting solution was centrifuged for 10 min at 15000 g, and the supernatant was aliquoted and stored at -80°C until further use. The lysate was used to measure the concentration of oxidative stress markers, antioxidants, inflammatory markers, BDNF, p-ERK, and p-CREB.

2.10. Measurement of oxidative stress markers, antioxidants, and NRF2

The oxidative stress markers such as malondialdehyde (MDA) and protein carbonyls (PC) and antioxidants such as catalase (CAT) and reduced glutathione (GSH) were measured from the hippocampal lysates using commercially available kits from Cayman chemicals (Arbor, MI). We also measured the transcription factor nuclear factor erythroid 2-related factor 2 (NRF2) from hippocampal lysates using a kit from Signosis (Santa Clara, CA). We followed the manufacturer's instructions for these assays. The total protein concentration in different tissue lysates was measured using a Pierce BCA reagent kit (Thermo Fisher Scientific, Waltham, MA), and the concentration of the markers was normalized with the total protein in respective tissue lysates.

2.11. Quantification of inflammatory markers, NLRP3, mitochondrial complex proteins, BDNF, p-ERK, and p-CREB

A cytokine array ELISA kit (Signosis) was employed for measuring various cytokines and chemokines in hippocampal tissue lysates. These comprised tumor necrosis factor-alpha ($\text{TNF-}\alpha$), vascular endothelial growth factor (VEGF), fibroblast growth factor-beta ($\text{FGF-}\beta$), interferon-gamma ($\text{IFN-}\gamma$), leptin, monocyte chemoattractant protein-1 (MCP-1), stem cell factor (SCF), macrophage inflammatory protein-1 alpha (MIP-1 α), interleukin-1 alpha (IL-1 α), IL-1 β , IL-5, IL-6, IL-15, IFN- γ inducible protein-10 (IP-10), regulated upon activation, normal T cell expressed and presumably secreted (rantes) and transforming growth factor- β (TGF- β). The protocols provided by manufacturers were followed for these assays. The protein concentration in the lysate was normalized to mg of protein. Changes observed for the proinflammatory markers $\text{TNF-}\alpha$ and $\text{IFN-}\gamma$ were validated further through well-standardized, commercially available ELISA kits (Signosis, detection range: 0.05-4000 pg/ml). The mitochondrial complex proteins I, II, III, and IV in hippocampal tissue lysates were measured using kits of MyBioSource (San Diego, CA) by following the manufacturer's protocols. The proteins involved in the NLRP3 inflammasome pathway were measured in hippocampal lysates using individual ELISA kits. These comprised

measurement of nuclear factor kappa B (NF- κ B; Aviva Systems Biology, San Diego, CA, detection range: 78–5000 pg/ml), NLRP3 (Aviva Systems Biology, detection range: 0.312–20 ng/ml), caspase-1 (BioVision Inc, Milpitas, CA), and IL-18 (R&D Systems, Minneapolis, MN, detection range, 62.5–4000 pg/ml). Commercially available kits were also used for measuring BDNF (Thermo Fisher Scientific, detection range, 12.29–3000 pg/mL), p-ERK1/2 (Enzo Life Sciences, Farmingdale, NY, detection range, 62.5–2000 pg/ml), and p-CREB (MyBioSource, detection range: 2.5–50 ng/ml).

2.12. Tissue processing and immunohistochemistry

We followed the previously published protocols for tissue processing and sectioning of fixed brain tissues using a cryostat [20–23,43,44]. Thirty-micrometer thick coronal sections were collected serially in 24-well plates containing phosphate buffer (PB) and stored at -20°C in cryobuffer until further use. Serial sections through the entire hippocampus were chosen in each animal belonging to different groups and processed for immunohistochemistry. Every 20th section was employed in immunohistochemical studies detecting the Ionized calcium-binding adaptor molecule 1 (IBA-1) positive microglia and glial fibrillary acidic protein (GFAP) positive astrocytes. Every 15th section was used in immunohistochemical studies visualizing doublecortin (DCX) positive newly born neurons. Immunohistochemical methods employed have been described in our previous reports [20,21,43]. The primary antibodies comprised goat anti-IBA-1 (1:1000, Abcam, Cambridge, MA), rabbit anti-GFAP (1:3000, Agilent Tech, Carpinteria, CA), and anti-DCX (1:300; Abcam). The secondary antibodies comprised horse biotinylated anti-goat IgG and goat biotinylated anti-rabbit IgG (1:250, Vector Labs, Burlingame, CA). The avidin-biotin complex reagent and the chromogen Vector gray were purchased from Vector Labs. The sections were mounted on subbed slides, counterstained with nuclear fast red (Vector Labs), processed for coverslipping using permount, and observed under a Nikon E600 microscope.

2.13. Evaluation of neuronal NRF2, astrocytes, microglia area, activated microglia, and newly born neurons

The presence of NRF2 in hippocampal neuronal nuclei was evaluated through NeuN and NRF2 dual immunofluorescence of brain tissue sections using mouse anti-NeuN (1:1000; Millipore, Darmstadt, Germany) and rabbit anti-NRF2 (1:500; Abcam), and Z-section analysis in a confocal microscope [23]. The hypertrophy of astrocytes in the dentate gyrus (DG) and hippocampal CA1 and CA3 subfields was evaluated by measuring area fractions occupied by GFAP immunoreactive structures using Image J (4 sections/subfield/animal, $n = 6/\text{group}$). NeuroLucida was employed for measuring the average area occupied by individual IBA-1+ microglial cells in the CA3 subfield (25–35 microglia in two sections/animal, $n = 6/\text{group}$). A dual immunofluorescence method was employed for visualizing microglia expressing both IBA-1 (a marker of all microglia) and ED-1 (CD68, a marker of activated microglia) in different regions of the hippocampus, using methods described in our earlier reports [20,22]. We used goat anti-IBA-1 (1:1000, Abcam), mouse anti-ED-1 (1:1000, Bio-Rad, Hercules, CA), donkey anti-goat IgG with Alexa Fluor 488 (1:200, Invitrogen, Waltham, MA) and donkey anti-mouse IgG with Alexa Fluor 594 (1:200, Invitrogen) in these studies. The percentages of microglia expressing IBA-1 and ED-1 were next quantified through Z-section analysis in a Nikon confocal microscope. The number of newly born DCX+ neurons in the subgranular zone-granular cell layer (SGZ-GCL) of the hippocampus was quantified using StereoInvestigator (MBF Bioscience, Williston, VT) using methods described in our earlier reports [43,45].

2.14. Quantification of NLRP3 inflammasome complex in microglia

The NLRP3 inflammasomes in microglia were visualized through

triple immunofluorescence for NLRP3, the apoptosis-associated speck-like protein containing a CARD (ASC), and IBA-1. The primary antibodies comprised goat anti-NLRP3 (1:500, Millipore, Burlington, MA), mouse anti-ASC (1:1000, Santa Cruz, Dallas, TX), and rabbit anti-IBA-1 (1:1000 Abcam). The secondary antibodies used were donkey anti-goat IgG Alexa Fluor 488 (1:200, Invitrogen), donkey anti-mouse Alexa Fluor 594 (1:200, Invitrogen), and anti-donkey rabbit Alexa Fluor 405 (1:200, Invitrogen). The sections were next examined through 2- μm thick, Z-section analysis using Leica THUNDER 3D Imager. The total number of NLRP3 inflammasomes (i.e., structures positive for both NLRP3 and ASC) per unit area ($\sim 216 \mu\text{m}^2$) of the CA3 subfield was measured using two sections per animal ($n = 6/\text{group}$). Also, the percentage of IBA-1+ microglia containing NLRP3 and ASC positive structures were measured.

2.15. Measurement of Syn+ and PSD95+ structures

The presynaptic and postsynaptic markers were visualized through dual immunofluorescence for synaptophysin (Syn) and postsynaptic density protein 95 (PSD95). The primary antibodies comprised anti-rabbit Syn (1:500, synaptic systems, Goettingen, Germany) and anti-goat PSD95 (1:500, Abcam). The secondary antibodies employed were donkey anti-rabbit IgG tagged Alexa Fluor 488 (1:200, Invitrogen) and donkey anti-goat IgG tagged Alexa Fluor 594 (1:200, Invitrogen). For measuring changes in Syn+ and PSD95+ puncta density in the dentate molecular layer (ML) and CA1 stratum radiatum, we employed 0.5- μm thick Z-sections using a Leica THUNDER 3D Imager. The area fraction of Syn+ and PSD95+ puncta were measured from randomly chosen 303 μm^2 areas in the dentate ML and the CA1 stratum radiatum (5 areas/region/animal, $n = 5\text{--}6/\text{group}$) using Image J.

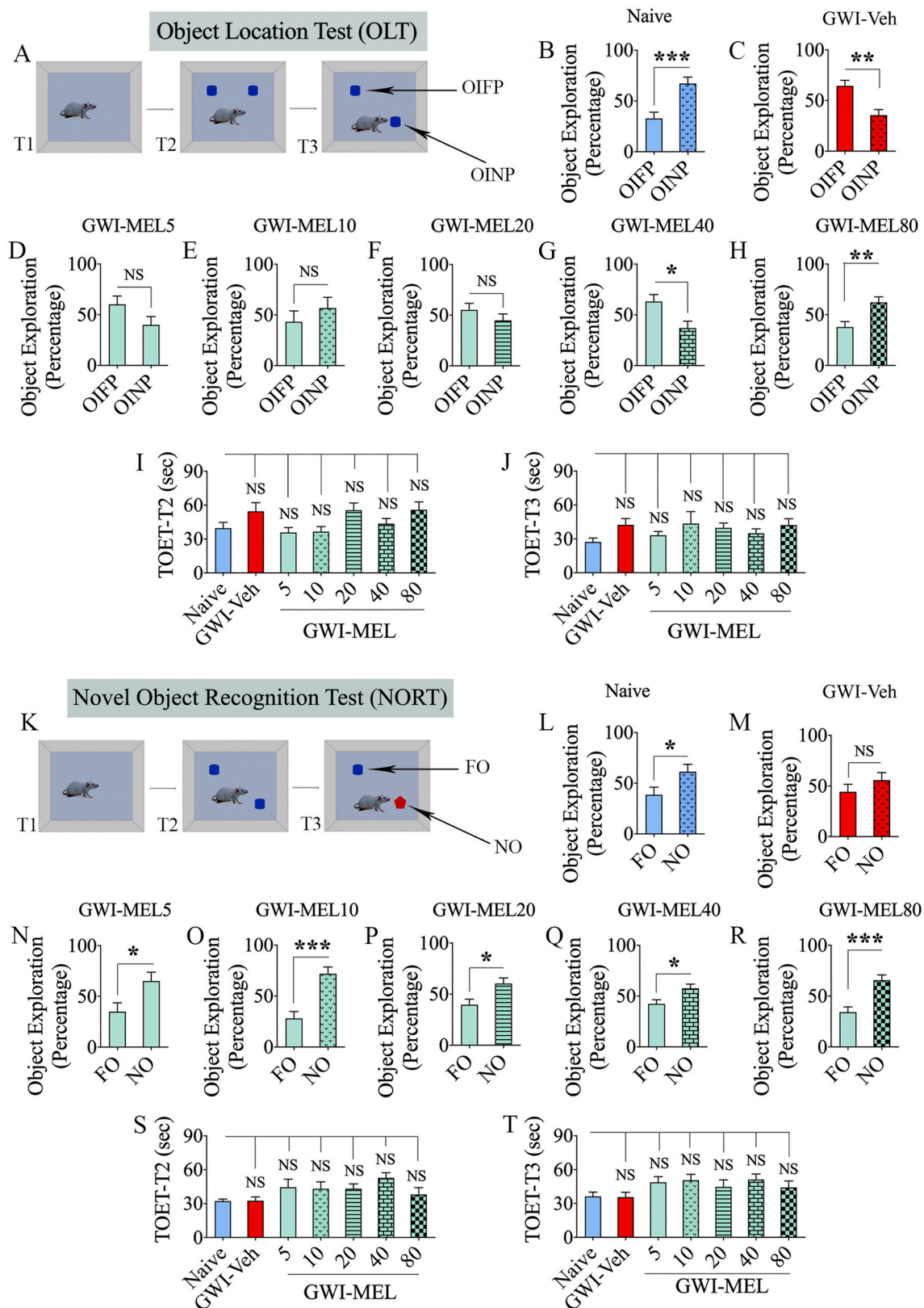
2.16. Statistical analysis

Two-tailed, unpaired, Student's *t*-test in the Prism software was employed to compare two data columns within groups in behavioral tests. The Mann-Whitney *U* test was employed when standard deviations between groups were statistically significant. One-way ANOVA with Student Neuman-Keuls post hoc tests was employed for comparisons involving three or more groups. The values mentioned in the bar charts are Mean \pm S.E.M., and $p < 0.05$ was considered statistically significant.

3. Results

3.1. MEL treatment at 80 mg/kg alleviated cognitive dysfunction in GWI rats

Cognitive ability to detect subtle changes in the environment, such as a minor change in the location of an object, was measured via an OLT [17]. Maintenance of this function rest on the integrity of the hippocampal tri-synaptic circuitry. This test's validity depends on the careful exploration of the position of objects in T2 (Fig. 2 [A]). Therefore, only animals that explored objects for ≥ 16 s in T2 and T3 were included for data analysis [21]. A majority of animals in every group met this criterion ($n = 10\text{--}14/\text{group}$ out of $15\text{--}16/\text{group}$). Naïve rats showed a higher affinity for the object in the novel place (OINP) over the object in the familiar place (OIFP) in T3 (Fig. 2 [B]). GWI rats that received vehicle displayed impairment in this cognitive task, as they explored the OIFP for more extended periods than the OINP ($p < 0.01$, $t = 3.7$ $df = 24$, Fig. 2[C]). In contrast, GWI rats that received MEL at 80 mg/kg ($p < 0.01$, $t = 2.8$ $df = 24$, Fig. 2[H]) spent significantly higher percentages of their object exploration time with the OINP, akin to the performance of naive control animals ($p < 0.001$, $t = 3.9$ $df = 20$, Fig. 2 [B]). GWI rats receiving low or moderate doses of MEL (5, 10, 20, or 40 mg/kg) remained impaired, however ($t = 0.9\text{--}2.7$, Fig. 2 [D-G]). ANOVA analyses revealed that the total object exploration times (TOETs) in T2 and T3 did not differ between groups ($p > 0.05$, $F = 1.1\text{--}2.3$, Fig. 2 [I-J]). The results suggest that MEL at a relatively higher dose (80 mg/kg) is



(caption on next page)

Fig. 2. MEL treatment improved hippocampus-dependent cognitive function and recognition memory in rats with chronic GWI. The cartoon and bar charts in the top three rows show the results of an object location test (OLT). Cartoon A depicts the various phases involved in the OLT whereas, the bar charts in B–H show the performance of animals belonging to naïve and GWI rats receiving vehicle (GWI-Veh) or different doses of MEL (GWI-MEL5, GWI-MEL10, GWI-MEL-20, GWI-MEL40, GWI-MEL80). The animals in the naïve group (B) preferred the object in the novel place (OINP) over the object in the familiar place (OIFP), implying their ability to discern minor changes in the environment. Animals in the GWI-Veh group (C) were impaired, as they preferred the OIFP over the OINP. Animals in the GWI-MEL5–40 groups (D–G) did not show improvement in cognitive function, whereas animals in the GWI-MEL80 group (H) behaved akin to the naïve control group, implying an improved cognitive function. The bar charts I–J compare the total object exploration times (TOETs) in trials 2 and 3 (T2, T3). The cartoon and bar charts in the lower three rows show the results of a novel object recognition test (NORT). Cartoon K shows the various phases involved in the NORT, whereas the bar charts in L–R show the performance of animals belonging to different groups. The animals in the naïve group (L) preferred the novel object (NO) over the familiar object (FO), suggesting their proficiency for object recognition memory. Animals in the GWI-Veh group (M) were impaired, as they did not prefer to explore the NO, whereas animals in the GWI-MEL5–80 groups (N–R) behaved similarly to the naïve control group, implying an improved recognition memory function. The bar charts S–T compare the TOETs in T2 and T3. *, $p < 0.05$, **, $p < 0.01$, and ***, $p < 0.001$; NS, not significant.

required for improving hippocampus-dependent cognitive function in rats afflicted with chronic GWI.

3.2. Object recognition memory in GWI rats improved with both low and moderate MEL doses

Recognition memory function in GWI rats was interrogated through a NORT (Fig. 2 [K]). Only animals that explored objects for ≥ 16 s in T2 and T3 ($n = 10$ –14/group out of 15–16/group) were included for data analysis. Naïve control animals explored the novel object for a significantly higher percentage of their object exploration time in T3 ($p < 0.05$, $t = 2.2$ $df = 22$, Fig. 2 [L]). GWI rats receiving vehicle displayed impaired recognition memory, consistent with our previous results [17, 21]. Worsened recognition memory was ostensible in these rats from their exploration of the familiar and novel objects for nearly equal percentages of the object exploration time ($p > 0.05$, $t = 1.1$ $df = 20$, Fig. 2 [M]). In divergence, GWI rats receiving low (5, 10, or 20 mg/kg) or moderate (40, or 80 mg/kg) doses of MEL spent significantly higher percentages of their object exploration time with the novel object ($p < 0.05$ –0.0001; $t = 2.5$ –4.6, $df = 18$ –26, Fig. 2 [N–R]). No differences were seen between groups for TOETs in both T2 and T3 ($p > 0.05$, $F = 1.5$ –1.9; Fig. 2 [S–T]). The behavior of MEL treated rats was comparable to the behavior of naïve control rats. These results imply that even a low dose of MEL therapy is sufficient for alleviating recognition memory impairment in rats with chronic GWI.

3.3. Both low and moderate doses of MEL improved spatial recognition memory in GWI rats

The recovery of spatial recognition memory in GWI rats after MEL treatment was evaluated through an OIPT (Fig. 3 [A]). The majority of the animals met the ≥ 14 s TOET criterion for T2 and T3 ($n = 8$ –15/group out of 10–16). In T3, naïve control rats showed the competence for making an association between objects and localities in which they were earlier discovered. Such behavior was evident from their predilection to investigate the two objects from T2 that swapped positions in T3 ($p < 0.05$, $t = 2.2$ $df = 14$, Fig. 3 [B]). The rats in the GWI-Veh group explored objects in familiar and novel locations for almost equal periods ($p > 0.05$, $t = 1.7$ $df = 26$, Fig. 3 [C]). In contrast, GWI rats that received MEL at 10, 20, 40, or 80 mg/kg examined the two objects from T2 that swapped positions in T3 for significantly higher percentages of their object exploration time ($p < 0.05$ –0.0001; $t = 2.1$ –8.4, $df = 26$ –28, Fig. 3 [E–H]), implying an ability for spatial recognition memory. GWI rats that received MEL at 5 mg/kg remained impaired, however ($p > 0.05$, $t = 0.8$ $df = 26$, Fig. 3 [D]). No differences were seen between groups for the TOETs in T2 and T3 ($p > 0.05$, $F = 2.0$ –2.5; Fig. 2 [I–J]). Thus, low dose MEL treatment is sufficient for reversing spatial recognition memory dysfunction in GWI rats.

3.4. Both low and moderate doses of MEL alleviated mood dysfunction in GWI rats

The extent of anhedonia was evaluated through an SPT (Fig. 3 [K]).

Naïve control rats clearly showed a preference for drinking sucrose-containing water over standard water ($p < 0.01$, $t = 3.3$ $df = 22$, $n = 12$, Fig. 3 [L]), which implied no anhedonia. The rats in the GWI-Veh group did not display such inclination as they drank standard and sucrose-containing water in almost comparable quantities ($p > 0.05$, $t = 1.4$, $df = 22$, $n = 12$, Fig. 3 [M]), denoting the manifestation of anhedonia in GWI rats. Remarkably, GWI rats that received different doses of MEL (5, 10, 20, 40, or 80 mg/kg) exhibited a liking for drinking sucrose-containing water over the standard water ($p < 0.05$ –0.0001, $t = 2.3$ –4.7, $n = 7$ –8/group, Fig. 3 [N–R]). ANOVA analysis revealed no significant differences between groups for the total liquid consumption ($p > 0.05$, $F = 1.2$, Fig. 3 [S]). Thus, mood function in rats with chronic GWI could be improved with a low dose of MEL therapy.

3.5. Immunohistochemical, biochemical, and molecular biological analyses of brain tissues

MEL's efficacy for reversing adverse cellular and molecular changes in the brain of GWI rats, the hippocampal tissues from various groups were processed for multiple immunohistochemical, biochemical, and molecular biological assays. Since the GWI-MEL5 group was not effective in improving hippocampus-dependent cognitive function in OLT and spatial recognition memory in OIPT, this group was not included for brain tissue analysis.

3.6. MEL modulated oxidative stress with enhanced antioxidants and NRF2 in GWI rats

We measured oxidative stress and antioxidant markers (MDA and PCs, NRF2, CAT, and GSH) to determine MEL's efficacy in reducing oxidative stress and recovering antioxidant status in chronic GWI ($n = 6$ /group). Evaluation using ANOVA showed differences between groups for MDA, PCs, NRF2, CAT, and GSH ($p < 0.05$ –0.0001, $F = 3.4$ –18.1, Fig. 4 [A–E]). In the GWI-Veh group, MDA and PCs were significantly increased compared to the naïve group ($p < 0.0001$, Fig. 4 [A–B]). In GWI-MEL10–80 groups, both MDA and PCs were significantly reduced compared to the GWI-Veh group ($p < 0.01$ –0.001, Fig. 4 [A–B]). The MDA amount was normalized to the naïve control concentration in MEL20–80 groups, whereas the intensity of PCs was regulated to the naïve control level in MEL10–40 groups and moved beneath the naïve control level in the MEL80 group (Fig. 4 [A–B]). The transcriptional regulator of antioxidant genes NRF2 was reduced in the GWI-Veh group compared to the naïve group ($p < 0.05$, Fig. 4 [C]). Reduced NRF2 observed at ~ 11 months post-exposure to GWI-related chemicals and stress in this study contrasted with the increased NRF2 seen at 4–6 months post-exposure in our previous studies [22,23]. The discrepancy in NRF2 levels between these studies likely reflects differences in time-points of analysis. Incessant oxidative stress and neuro-inflammation have likely suppressed the compensatory NRF2 response at extended time-points after exposure to GWI-related chemicals and stress. Remarkably, MEL therapy at 20–80 mg/kg normalized to naïve control levels ($p > 0.05$, Fig. 4 [C]). Furthermore, elevated levels of oxidative stress markers in the GWI-Veh group were associated with a

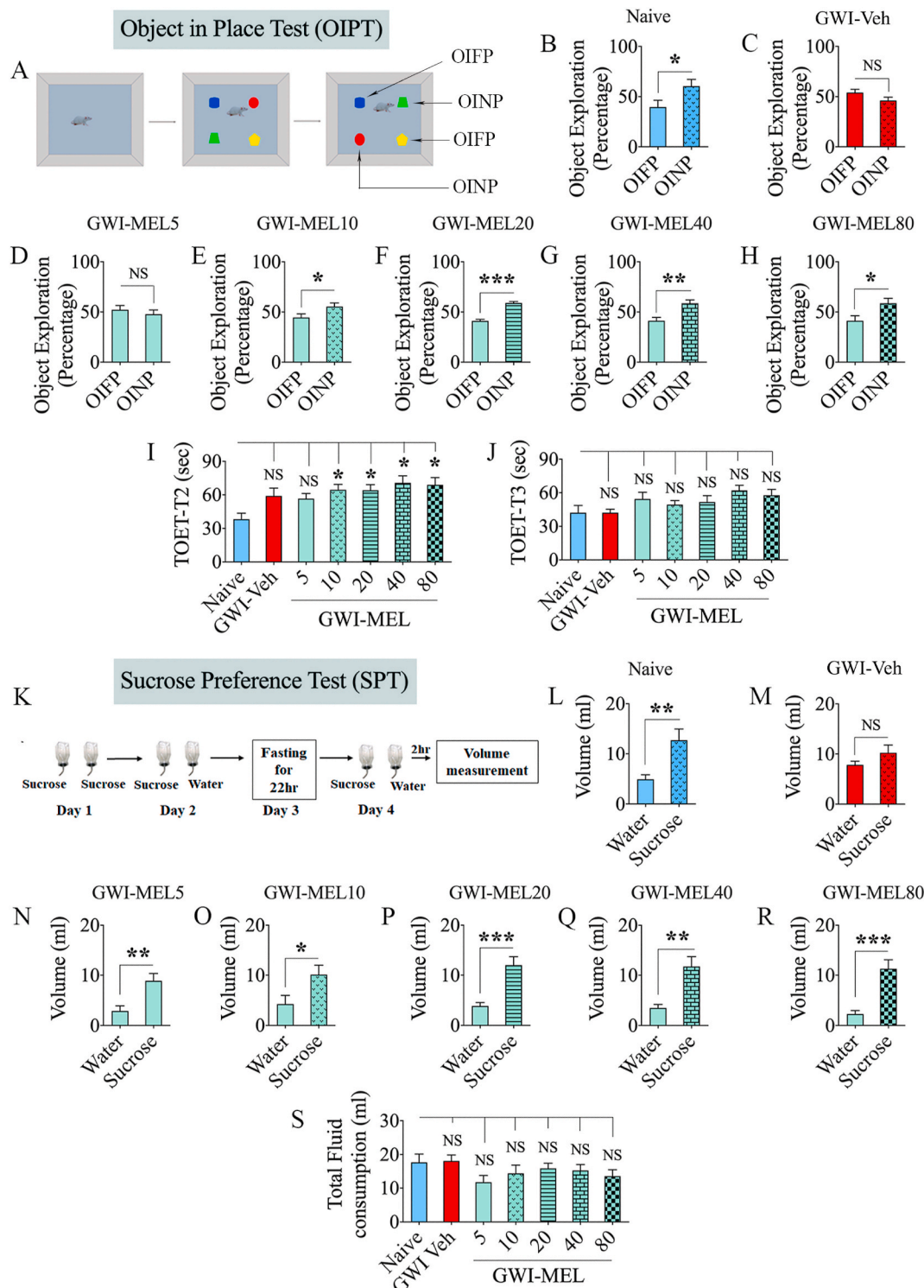


Fig. 3. MEL treatment improved associative recognition memory function and reversed anhedonia in rats with chronic GWI. The cartoon and bar charts in the top three rows show the results of an object-in-place test (OIPT). Cartoon A shows the various phases involved in the OIPT whereas, the bar charts in B–H show the performance of animals belonging to naïve and GWI rats receiving vehicle (GWI-Veh group) or MEL (GWI-MEL5–80 groups). The animals in the naïve group (B) preferred objects in the novel place (OINP) over the objects in the familiar place (OIFP), implying their ability for associative recognition memory. Animals in the GWI-Veh group (C) and GWI-MEL5 group (D) were impaired, as they preferred the OIFP over the OINP, whereas animals in the GWI-MEL10–80 groups (E–H) behaved similarly to the naïve control group, implying an improved associative recognition memory function. The bar charts I–J compare the total object exploration times (TOETs) in trials 2 and 3 (T2, T3). The cartoon K and bar charts L–S in the lower three rows illustrate the experimental design and findings of a sucrose preference test (SPT). Animals in the naïve group (L) preferred sucrose-containing water over the standard water. Animals in the GWI-Veh group (M) exhibited anhedonia as they did not show an increased propensity for drinking the sucrose-containing water over the standard water. In contrast, animals in the GWI-MEL5–80 groups displayed a predilection to drink the sucrose-containing water (N–R), implying no anhedonia. The bar chart in S shows that the total fluid consumption did not differ between groups. *, $p < 0.05$, **, $p < 0.01$, and ***, $p < 0.001$; NS, not significant.

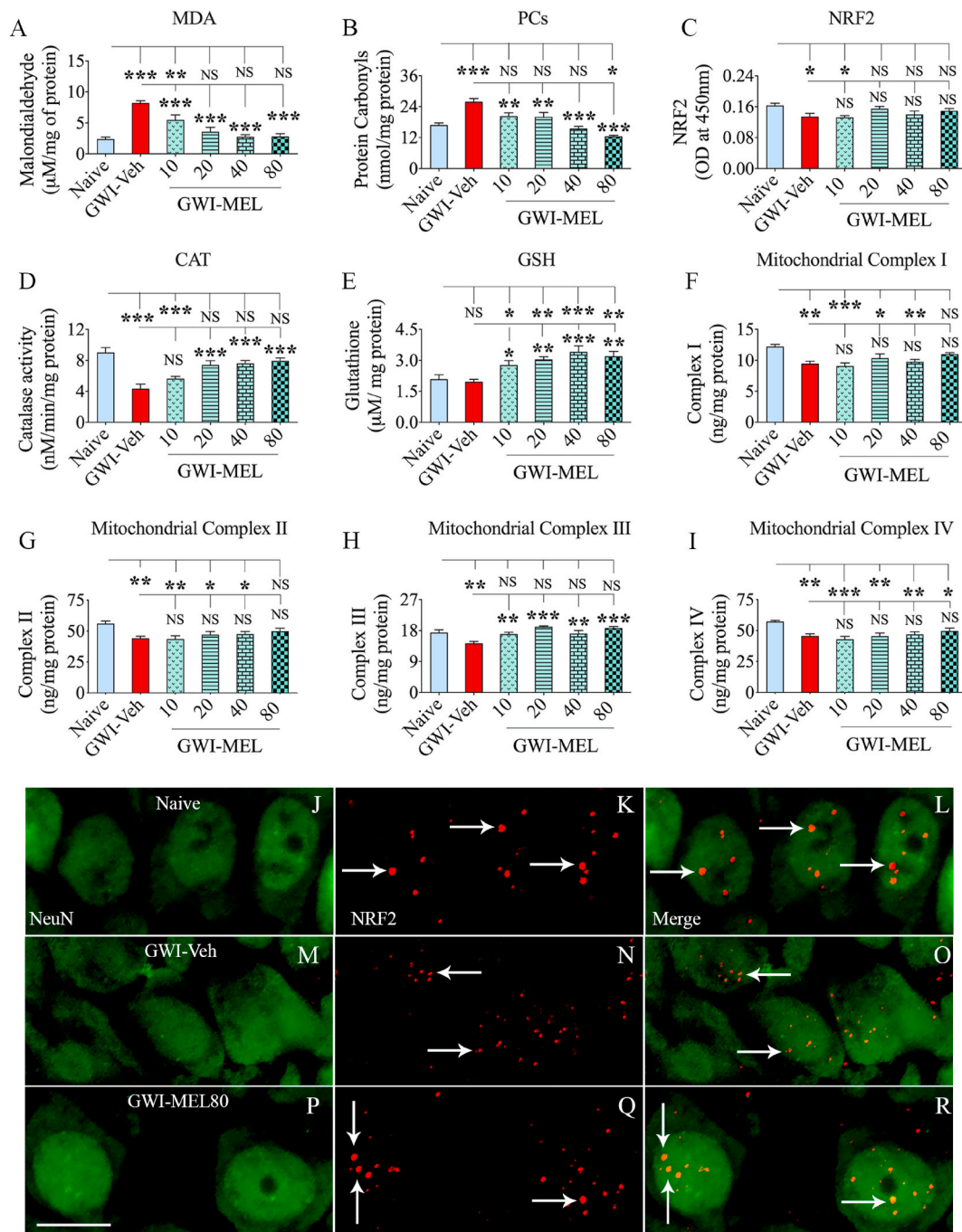


Fig. 4. MEL treatment to rats with chronic GWI reduced oxidative stress, improved antioxidant status and mitochondrial function in the hippocampus. The bar charts in A-E compare the concentration of malondialdehyde (MDA; A), protein carbonyls (PCs; B), the nuclear factor erythroid 2-related factor 2 (NRF2; C), catalase (CAT; D), and glutathione (GSH; E) in the hippocampus between naïve, and GWI rats receiving vehicle (GWI-Veh) or different doses of MEL (GWI-MEL10-80 groups). Note that MDA and PCs were upregulated, and NRF2 and CAT were downregulated in the GWI-Veh group, compared to the naïve control group. In all GWI-MEL groups, MDA and PCs were reduced compared to the GWI-Veh group. NRF-2 and CAT levels in the GWI-MEL20-80 groups were normalized to the naïve control level, whereas the GSH concentration in the GWI-MEL10-80 groups increased above the level seen in both naïve and GWI-Veh groups. The bar charts in F-I compare the concentration of mitochondrial complexes I-IV in the hippocampus between different groups. All complexes were reduced in the GWI-Veh group compared to the naïve control group. The complex I (F) and II (G) were normalized to the naïve control level in the GWI-MEL80 group, and the complex III (H) was normalized to the naïve control level in the GWI-MEL10-80 groups. Figures J-R illustrate the presence of NRF-2 in the nuclei of CA3 pyramidal neurons from naïve control (J-L), GWI-Veh (M – O), and GWI-MEL80 (P-R) groups. Scale bar, 12.5 μm *, p < 0.05, **, p < 0.01, and ***, p < 0.001; NS, not significant.

decreased level of the antioxidant CAT ($p < 0.001$, Fig. 4 [D]). Low and moderate doses of MEL (20–80 mg/kg) normalized the CAT activity to naïve control levels and raised above the GWI-Veh group level ($p < 0.001$, Fig. 4 [D]). Besides, rats in the GWI-MEL10-80 groups showed significantly enhanced GSH levels than both naïve and GWI-Veh groups ($p < 0.05$ –0.001, Fig. 4 [E]). The evaluation of NRF2 in CA3 pyramidal

neurons through NeuN and NRF2 dual immunofluorescence and Z-section confocal microscopy also suggested reduced levels of NRF2 in the nuclei of neurons from the GWI-Veh group, compared to the naïve control group (Fig. 4 [J-O]). Notably, the speckles of NRF2 staining were smaller in size and not present in all neurons in the GWI-Veh group. In contrast, the extent of neuronal NRF2 stained speckles appeared

comparable between naïve control and MEL80 groups in terms of density and size (Fig. 4 [J-L, P-R]). Thus, MEL's protective effect against increased oxidative stress in the hippocampus of GWI rats appeared to be mediated through robust antioxidant activity and normalization of NRF2 activity.

3.7. MEL normalized mitochondrial complex proteins in GWI rats

ANOVA showed significant differences in the various mitochondrial complex proteins between groups ($p < 0.01-0.001$, $F = 4.1-7.3$, $n = 6/\text{group}$). Post-hoc analysis revealed that all mitochondrial complex

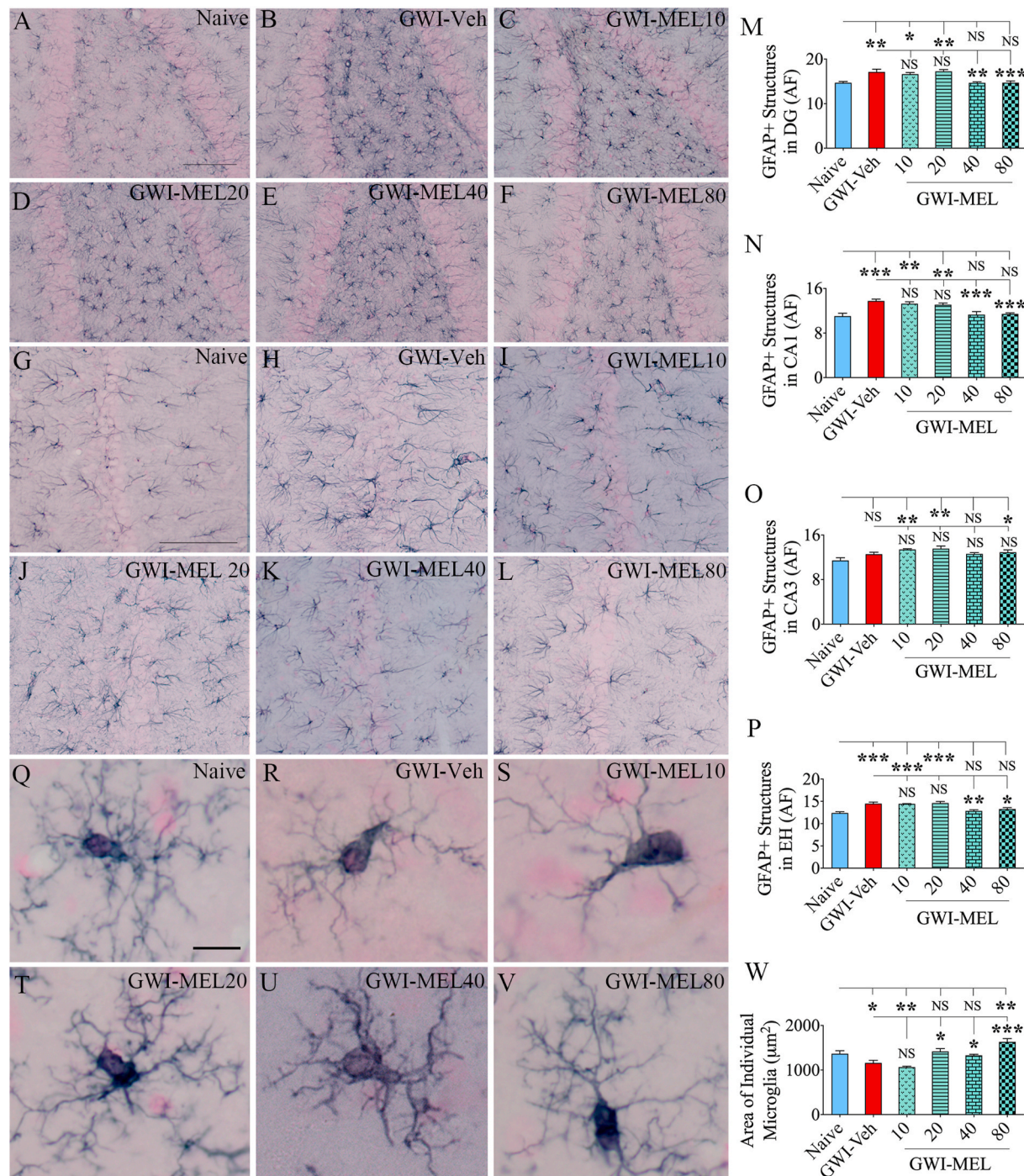


Fig. 5. MEL treatment to rats with chronic GWI diminished astrocyte hypertrophy and modulated microglial phenotype in the hippocampus. Figures A–L illustrate examples of GFAP+ astrocytes from the DG (A–F) and the CA1 subfield (G–L) of naïve control (A, G), GWI-Veh (B, H), GWI-MEL (C–F, I–L) groups. The bar charts M – P compare the area fraction (AF) of GFAP + structures in the DG (M), the CA1 subfield (N), the CA3 subfield (O), and the entire hippocampus (EH; P) between different groups. AF's of GFAP + structures were higher in the GWI-Veh group in all hippocampal regions but normalized to the naïve control level in the DG and CA1 subfields and when the hippocampus was taken in entirety in the GWI-MEL40 and GWI-MEL80 groups. Figures Q–V illustrate the morphology of representative IBA-1+ microglia from the CA3 subfield of naïve control (Q), GWI-Veh (R), GWI-MEL10-80 groups (S–V). The bar chart W compares the area occupied by individual IBA-1+ microglia in the CA3 subfield of different groups. Compared to the naïve control group, individual microglia was diminished in the GWI-Veh group, normalized in the GWI-MEL10-40 groups, and enhanced in the GWI-MEL80 group. Scale bar, A–L = 100 μm ; Q–V = 10 μm . *, $p < 0.05$; **, $p < 0.01$; ***, $p < 0.001$; NS, not significant.

proteins (complex I, II, III, and IV) were reduced in the GWI-Veh group compared to the naïve group ($p < 0.01$, Fig. 4 [F–I]), implying hypo-function of mitochondria in the hippocampus at ~11 post-exposure to GWI chemicals and stress. This finding diverged with the hyperactive mitochondria observed at 6 months post-exposure in our previous study [23]. A shift from hyperactive to hypoactive status likely reflects decreased antioxidant and NRF2 levels with the disease progression, as such changes could further enhance the oxidative stress and affect the transcription and translation of mitochondrial complex protein subunits. The complex III protein was normalized to naïve control levels in GWI-MEL10-80 groups ($p > 0.05$, Fig. 4 [H]). The complex I and II were also normalized to naïve control levels in the GWI-MEL80 group ($p > 0.05$, Fig. 4 [F–G]). However, MEL treatment did not improve the level of complex IV protein. At all doses of MEL, complex IV levels remained less than the naïve control group ($p < 0.05–0.001$, Fig. 4 [I]). The results suggested that low to moderate MEL doses could improve complex III, whereas both low and moderate doses could improve the levels of complex I and II in the brain of GWI rats.

3.8. MEL treatment reduced astrocyte hypertrophy in the hippocampus of GWI rats

Examples of astrocytes' distribution and morphology in the DG and CA1 subfields of the hippocampus from different groups are illustrated (Fig. 5 [A–L]). Compared to the naïve group, the GWI-Veh group displayed increased GFAP + astrocytic elements (Fig. 5 [A–B, G–H]), implying the occurrence of astrocyte hypertrophy, a sign of chronic inflammation. The area occupied by GFAP + astrocytic elements were measured using J-image ($n = 5–6$ /group). The divergences between groups were significant for all subfields of the hippocampus and when the hippocampus was taken in totality ($p < 0.01–0.0001$, $F = 4.3–12.3$, Fig. 5 [M – P]). The differences were significant for DG and CA1 subfields and the entire hippocampus ($p < 0.01–0.001$, Fig. 5 [M – N, P]). GWI rats receiving MEL treatment at 40–80 mg/kg doses displayed significantly reduced hypertrophy of astrocytes than the GWI-Veh group in these regions ($p < 0.05–0.001$, Fig. 5 [M – N, P]). The extent of astrocyte hypertrophy remained comparable to the GWI-Veh group in GWI-MEL10-20 groups, however ($p > 0.05$, Fig. 5 [M – N, P]). MEL did not reduce GFAP+ structures in the hippocampus's CA3 subfield (Fig. 5 [O]). Thus, MEL treatment at moderate doses (40–80 mg/kg) effectively lowered the overall astrocyte hypertrophy in the hippocampus.

3.9. MEL diminished activated microglia and normalized microglial phenotype in GWI rats

We measured the area occupied by individual microglia in the CA3 subfield of the hippocampus ($n = 6–7$ /group) to understand the phenotypic changes, which revealed differences between groups ($p < 0.0001$, $F = 12.6$, Fig. 5 [Q–W]). Naïve control rats displayed individual microglia occupying a relatively more significant area of the brain tissue (Fig. 5 [Q]). Such changes were mainly due to a large number of highly ramified processes. GWI rats, in contrast, exhibited individual microglia occupying reduced areas of the brain tissue due to a reduced number of processes as well as the loss of extensive ramification of processes, which are features of moderately activated microglia ($p < 0.05$, Fig. 5 [R, W]). GWI-MEL10 group also showed reduced microglia processes as the GWI-Veh group ($p > 0.05$, Fig. 5[S, W]). However, GWI-MEL20-80 groups exhibited normalized microglia morphology with highly ramified processes. The average areas of the brain tissue occupied by individual microglia in the GWI-MEL20-40 groups were comparable to the naïve control group ($p > 0.05$, Fig. 5 [T–U, W]). Notably, the GWI-MEL80 group displayed highly ramified microglia that occupied more area of the brain tissue than microglia in the naïve group ($p < 0.01$, Fig. 5 [V, W]).

Next, we investigated the extent of activated microglia in different groups via IBA-1 and ED-1 dual immunofluorescence ($n = 5$ /group).

Examples of IBA-1+ microglia expressing ED-1 in the CA3 subfield of the hippocampus from different groups are illustrated (Fig. 6 [A–R]). Compared to the naïve control group, the GWI-Veh group displayed increased percentages of IBA-1+ microglia with ED-1+ structures (i.e., activated microglia) in the hippocampus, implying the presence of chronic neuroinflammation. The differences were significant for all subfields of the hippocampus and the entire hippocampus ($p < 0.01–0.0001$, $F = 5.8–22.2$, Fig. 6 [S–V]). MEL treatment at 40–80 mg/kg significantly reduced the percentages of activated microglia in the DG and the CA3 subfields, and the entire hippocampus ($p < 0.01–0.001$, Fig. 6 [S–T, V]). Compared to the GWI-Veh group, GWI-MEL10-20 groups did not display reduced percentages of activated microglia, however ($p > 0.05$, Fig. 6 [S–T, V]).

3.10. MEL treatment inhibited NLRP3 inflammasome formation in GWI rats

We quantified the extent of NLRP3 inflammasomes in the hippocampus to comprehend the potential mechanisms by which MEL alleviated neuroinflammation ($n = 6$ /group). Examples of microglia displaying NLRP3 inflammasomes in different groups are illustrated (Fig. 7 [A–R]). We first quantified the concentrations of NF- κ B, NLRP3, caspase-1, all of which showed differences between groups ($F = 3.9–14.1$, $p < 0.01–0.0001$, Fig. 7 [S–U]). NF- κ B, NLRP3, and caspase-1 were elevated in the GWI-Veh group compared to the naïve group ($p < 0.05–0.001$). Compared to the GWI-Veh group, NF- κ B and Caspase-1 were significantly reduced in the GWI-MEL40-80 groups ($p < 0.05–0.001$, Fig. 7 [S, U]), whereas NLRP3 was reduced in GWI-MEL20-80 groups with the amount going below the naïve control level in the GWI-MEL80 group ($p < 0.05–0.001$, Fig. 7 [T]). ANOVA analyses of the amount of NLRP3-ASC complex (a measure of active inflammasome complex) and percentages of microglia with the NLRP3-ASC complex in the CA3 subfield of the hippocampus showed differences between groups ($p < 0.01–0.001$; $F = 4.6–13.5$, Fig. 7 [V–W]). Notably, all doses of MEL examined in the study (i.e., 10–80 mg/kg) were able to reduce the occurrence of NLRP3 inflammasomes. Both the number of inflammasomes per unit area and the percentage of microglia with NLRP3 inflammasomes were significantly reduced in the GWI-MEL10-80 groups compared to the GWI-Veh group ($p < 0.01–0.001$, Fig. 7 [V–W]). Quantification of IL-18 and IL-1 β (the end products of NLRP3 inflammasomes) also showed differences between groups ($p < 0.01–0.001$; $F = 5.4–24.4$). Increased occurrence of inflammasomes correlated with a significantly higher level of IL-18 in the GWI-Veh group ($p < 0.001$), whereas reduced levels of inflammasomes in GWI-MEL10-80 groups were associated with significantly reduced concentrations of IL-18 compared to the GWI-Veh group ($p < 0.001$, Fig. 7 [X]). The IL-1 β concentration was also reduced in the GWI-MEL40-80 groups compared to the GWI-Veh group (Fig. 8 [Y]). Thus, MEL treatment robustly inhibited NLRP3 inflammasome formation in microglia and neurons in GWI rats.

3.11. MEL treatment reduced several other proinflammatory proteins in GWI rats

We measured multiple proinflammatory cytokines and chemokines to discern the effects of MEL intervention on neuroinflammation in the hippocampus of rats with chronic GWI using a cytokine array ($n = 6$ /group). ANOVA analysis showed significant differences between groups for levels of TNF- α , IFN- γ , MCP-1, and MIP-1 α ($F = 6.1–9.7$, $p < 0.01–0.0001$, Fig. 7 [Z–AC]). The post-hoc analysis demonstrated significant upregulation of TNF- α , IFN- γ , MCP-1, and MIP-1 α in the GWI-Veh group compared to the naïve control group ($p < 0.05$, Fig. 7 [Z–AC]). All doses of MEL examined were able to significantly reduce the concentration of TNF- α and IFN- γ in the hippocampus of GWI rats ($p < 0.05–0.001$, Fig. 7 [Z–AA]). MCP-1 and MIP-1 α were also reduced in the GWI-MEL40-80 groups compared to the GWI-Veh group ($p <$

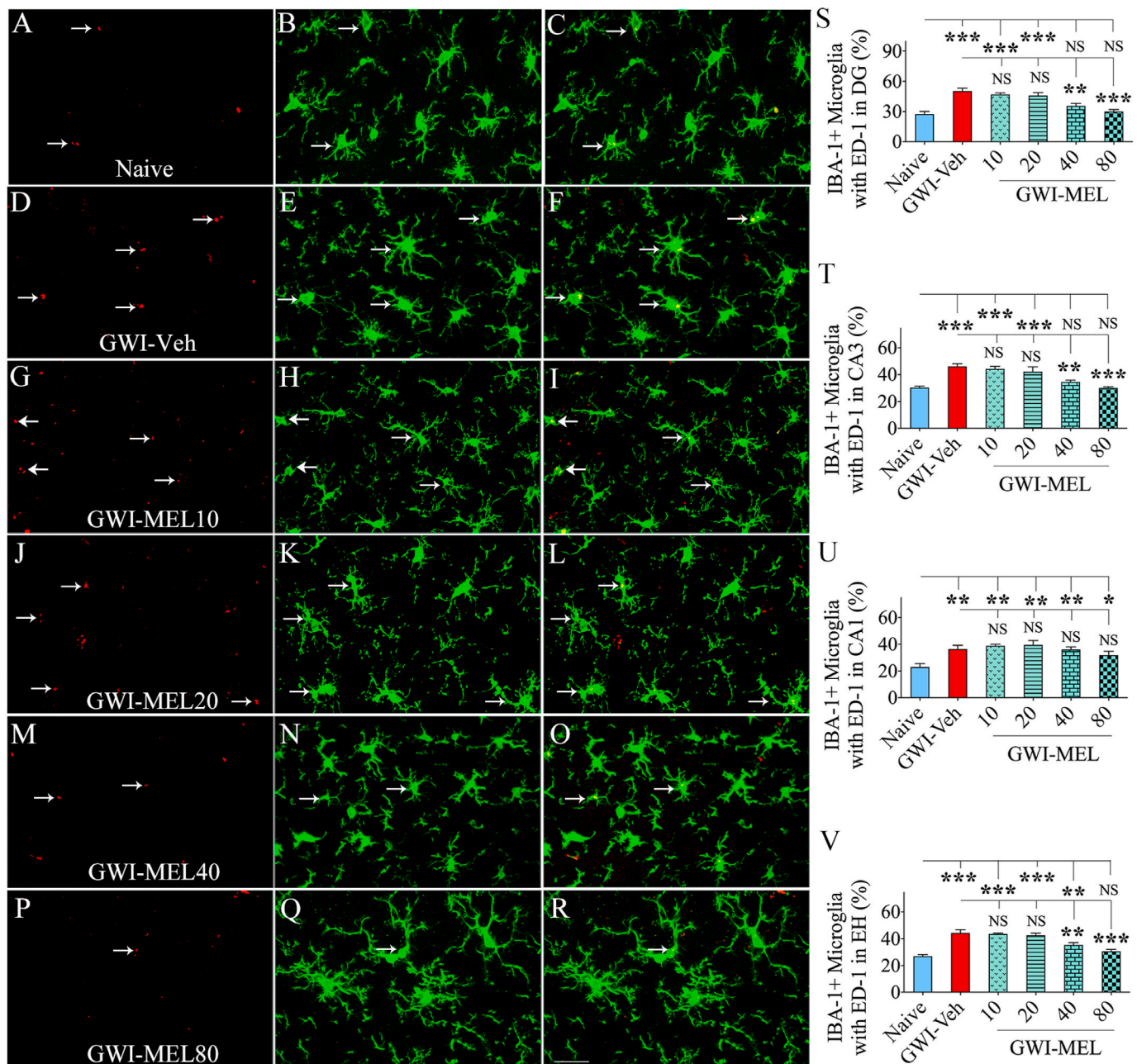
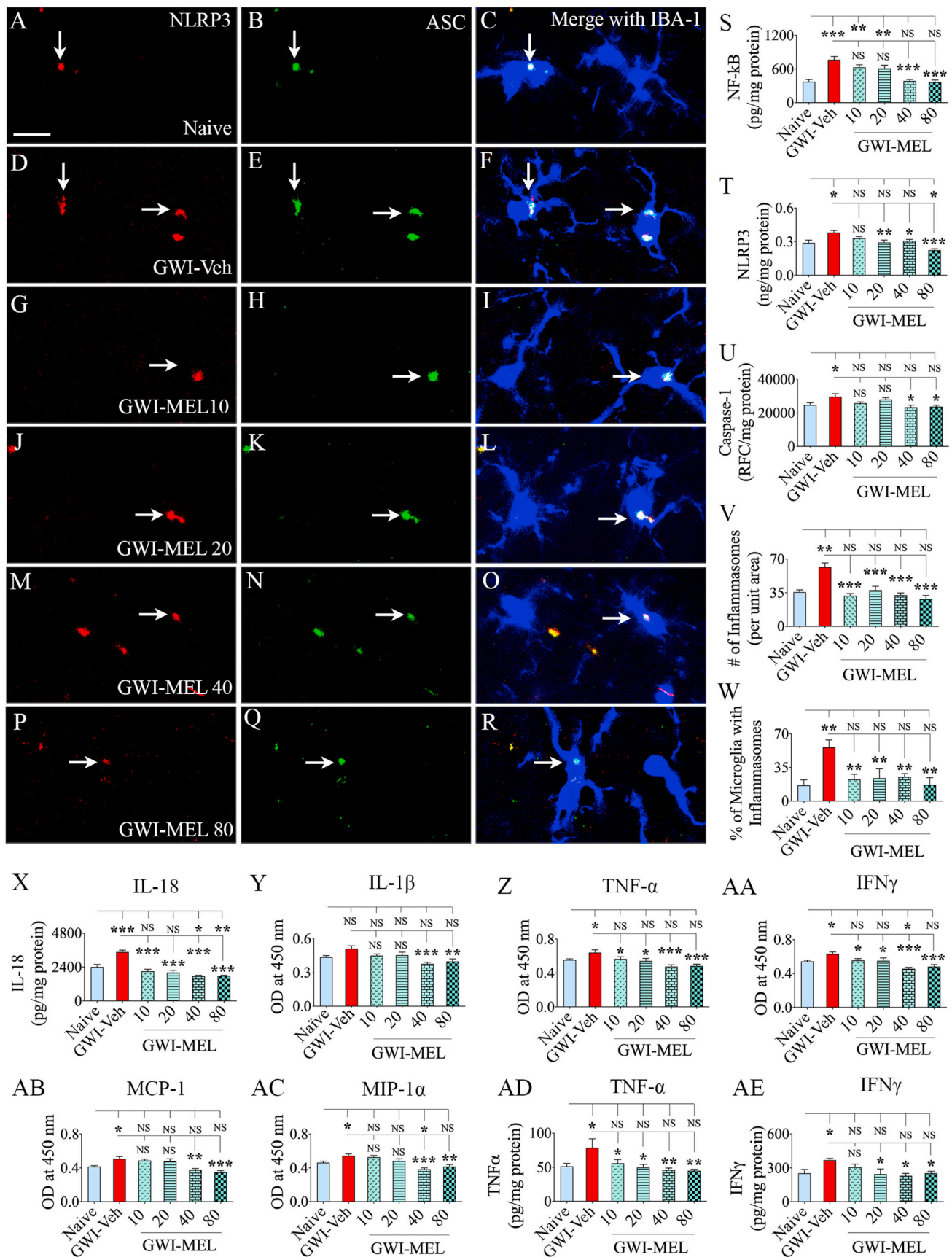


Fig. 6. MEL treatment to rats with chronic GWI reduced activated microglia in the hippocampus. Figures A–R illustrate examples of IBA-1+ microglia displaying ED-1+ structures (i.e., activated microglia) from the CA3 subfield of naïve control (A–C), GWI-Veh (D–F), GWI-MEL10 (G–I), GWI-MEL20 (J–L), GWI-MEL40 (M–O), GWI-MEL80 (P–R) groups. The bar charts S–V compare percentages of IBA-1+ microglia with ED-1 in the DG (S), the CA3 subfield (T), the CA1 subfield (U), and the entire hippocampus (V) between different groups. The percentages of activated microglia were higher in the GWI-Veh group than the naïve control group in all hippocampal regions but significantly reduced in the DG and CA3 subfields and the entire hippocampus in the GWI-MEL40 and GWI-MEL80 groups. Scale bar, A–R = 25 μ m; *, $p < 0.05$, **, $p < 0.01$, and ***, $p < 0.001$; NS, not significant.

0.01–0.001, Fig. 7 [AB–AC]). TNF- α and IFN- γ were further validated through quantitative ELISA, which showed differences between groups ($p < 0.05$ –0.01, $F = 3.3$ –3.8, Fig. 7 [AD–AE]). The post-hoc analysis revealed that the concentration of TNF- α and IFN- γ were significantly increased in the GWI-Veh group ($p < 0.05$, Fig. 7 [AD–AE]). Compared to the GWI-Veh group, the concentration of TNF- α was reduced in the MEL10–80 groups ($p < 0.05$ –0.01, Fig. 7 [AD]), whereas the concentration of IFN- γ was reduced in the MEL20–80 group ($p < 0.05$, Fig. 7 [AE]). Thus, MEL therapy reduced the concentration of TNF- α , IFN- γ , MCP-1, and MIP-1 α in the hippocampus, with the most significant effects at 40–80 mg/kg doses.

3.12. MEL treatment improved hippocampal neurogenesis in GWI rats

Examples of DCX+ newly born neurons in the hippocampus from different groups are illustrated (Fig. 8 [A–F]). We quantified the number of DCX+ newly born neurons in the SGZ-GCL of the hippocampus using stereology (Fig. 8 [G]). Such quantification provided information on the status of hippocampal neurogenesis with Veh or MEL treatment in GWI rats. The GWI-Veh group exhibited decreased production of newly born neurons compared to the naïve control group ($p < 0.05$, Fig. 8 [G]). In contrast, GWI rats receiving MEL at 80 mg/kg displayed DCX+ new neuron numbers that were comparable to naïve control rats ($p > 0.05$, Fig. 8 [G]). However, the extent of neurogenesis in GWI-MEL10–40



(caption on next page)

Fig. 7. MEL treatment to rats with chronic GWI diminished NLRP3 inflammasomes and reduced the concentration of multiple proinflammatory markers in the hippocampus. Figures A–R illustrate examples of NLRP3 inflammasomes in IBA-1+ microglia from the CA3 subfield of naïve control (A–C), GWI-Veh (D–F), GWI-MEL10 (G–I), GWI-MEL20 (J–L), GWI-MEL40 (M – O), GWI-MEL80 (P–R) groups. The bar charts in S–X compare concentrations of NF-kB (S), NLRP3 (T), caspase-1 (U), the number of inflammasomes/unit area (V), the percentage of microglia with inflammasomes (W), and IL-18 (X). These measures were upregulated in the GWI-Veh group but normalized to naïve control levels in the GWI-MEL groups. NF-kB was normalized in the GWI-MEL40-80 groups. NLRP3 was normalized in the GWI-MEL10-40 groups and reduced below the naïve control level in the GWI-MEL80 group. Caspase-1, the number of inflammasomes per unit area, and the percentage of microglia with inflammasomes were normalized in GWI-MEL10-80 groups. IL-18 was normalized in the GWI-MEL10-20 groups and reduced below the naïve control level in GWI-MEL40-80 groups. The bar charts in Y–AC compare the concentration of interleukin-1 beta (IL-1β; Y), tumor necrosis factor-alpha (TNF-α, Z), interferon-gamma (IFN-γ; AA), monocyte chemoattractant protein-1 (MCP-1; AB), macrophage inflammatory protein 1 alpha (MIP-1α; AC) between different groups assessed through a cytokine array. The bar charts AD-AE compare TNF-α (AD) and IFN-γ (AE) concentrations between different groups measured through individual ELISA. Compared to the naïve control group, TNF-α, IFN-γ, MCP-1, and MIP-1α were upregulated in the GWI-Veh group but normalized or reduced below the naïve control level in the GWI-MEL10-80 group. The concentration of IL-1β was reduced in the GWI-MEL40-80 groups compared to the GWI-Veh group. Scale bar, A–R = 25 μm; *, p < 0.05, **, p < 0.01, and ***, p < 0.001; NS, not significant.

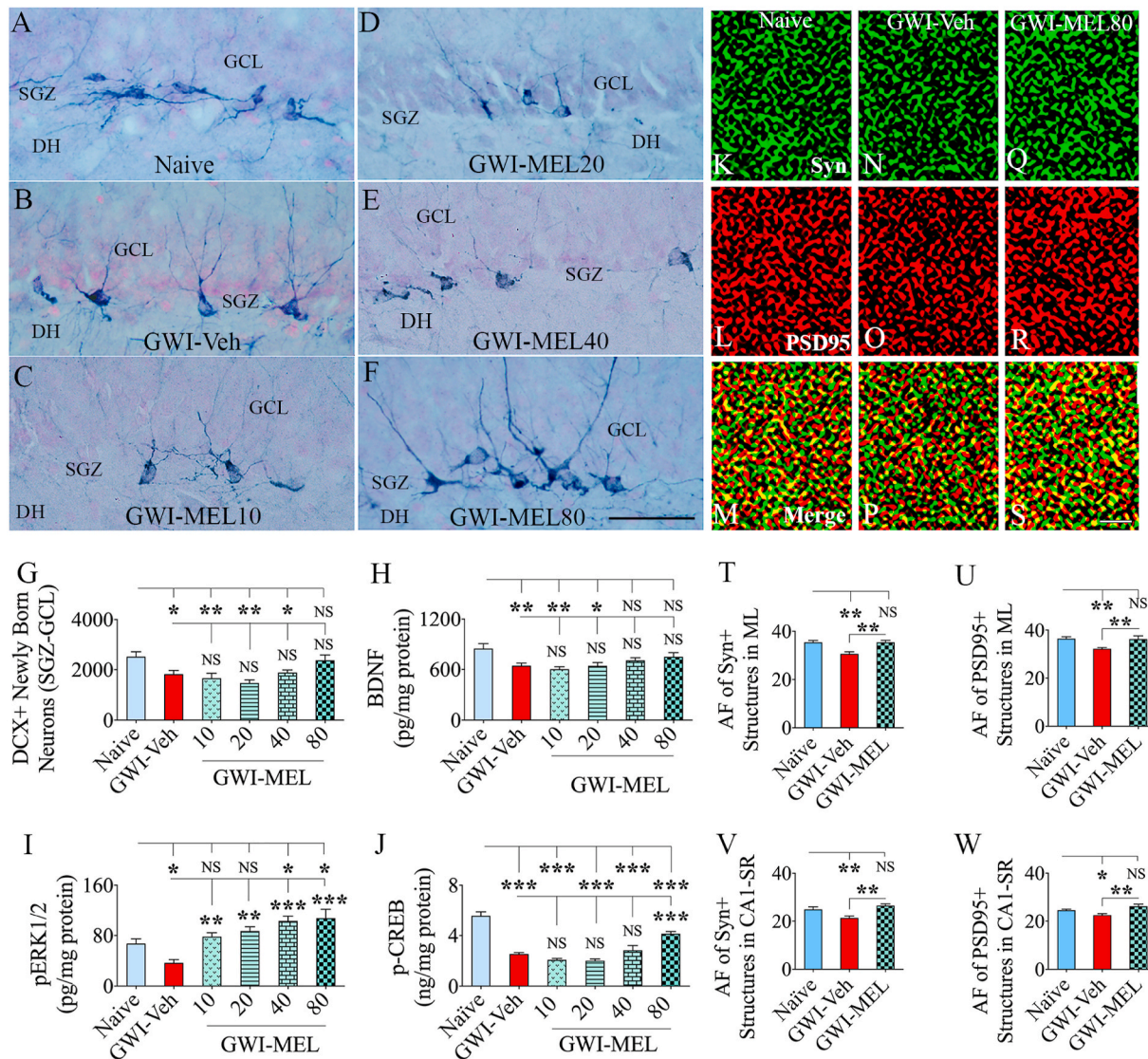


Fig. 8. MEL treatment in rats with chronic GWI enhanced neurogenesis, activated BDNF-ERK-CREB pathway, and reduced synapse loss in the hippocampus. Figures A–F illustrate examples of doublecortin-positive (DCX+) newly born neurons from naïve control (A), GWI-Veh (B), GWI-MEL10 (C), GWI-MEL20 (D), GWI-MEL40 (E), GWI-MEL80 (F) groups. The bar chart G compares the number of DCX+ neurons between different groups. Neurogenesis was decreased in the GWI-Veh group but normalized in the GWI-MEL80 group. GCL, granule cell layer; SGZ, subgranular zone. Scale bar, A–F = 50 μm. The bar charts H–J compare the concentration of BDNF (H) pERK1/2 (I) and p-CREB (J) between different groups. The concentration of all these proteins was decreased in the GWI-Veh group but normalized to the naïve control level in GWI-MEL groups. BDNF was normalized in the GWI-MEL40-80 groups, pERK1/2 was normalized in the GWI-MEL10-20 groups and went above the naïve control level in GWI-MEL40-80 groups. The concentration of p-CREB did not normalize to the naïve control level but significantly increased in the GWI-MEL80 group compared to the GWI-Veh group. Figures K–S shows examples of synaptophysin+ (Syn+) and postsynaptic density 95+ (PSD95+) puncta in the dentate molecular layer from naïve control (K–M), GWI-Veh (N–P), GWI-MEL80 (Q–S) groups. The bar charts T–W compare area fraction (AF) of Syn+ and PSD95+ puncta in the dentate molecular layer (T–U) and CA1 subfield (V–W) between different groups. Both Syn+ and PSD95+ puncta were reduced in the GWI-Veh group and normalized to the naïve control level in the GWI-MEL80 group. Scale bar, K–S = 1 μm; *, p < 0.05, **, p < 0.01, and ***, p < 0.001; NS, not significant.

groups remained less than the naïve control group ($p < 0.05$ – 0.01 , Fig. 8 [G]). Thus, 80/mg/Kg dose of MEL normalized hippocampal neurogenesis in GWI rats.

3.13. MEL enhanced the BDNF-ERK-CREB signaling pathway in the hippocampus of GWI rats

We measured BDNF, pERK1/2, and p-CREB in the hippocampus to understand the potential mechanism underlying MEL-mediated improved cognitive function in rats with chronic GWI. Notably, the concentration BDNF, pERK1/2, and p-CREB differed significantly between groups ($p < 0.01$ – 0.0001 , $F = 4.8$ – 36.2 , Fig. 8 [H–J]). BDNF concentration was reduced in the hippocampus of rats GWI-Veh group compared to the naïve group ($p < 0.01$, Fig. 8 [H]). MEL treatment at 40–80 mg/kg normalized the BDNF concentration to naïve control levels ($p > 0.05$, Fig. 8 [H]). Furthermore, the GWI-Veh group displayed a reduced concentration of pERK1/2 compared to the naïve control group ($p < 0.05$, Fig. 8 [I]). MEL treatment at 10–80 mg/kg enhanced the concentration of pERK1/2 compared to the GWI-Veh group ($p < 0.01$ – 0.001 , Fig. 8 [I]). Compared to the naïve control group, pERK1/2 concentration normalized with 10–20 mg/kg doses of MEL ($p > 0.05$) and further increased with 40–80 mg/kg doses of MEL ($p < 0.05$, Fig. 8 [I]). Moreover, a reduced concentration of p-CREB was seen in the GWI-Veh group compared to the naïve group ($p < 0.001$, Fig. 8 [J]), which did not change significantly with 10–40 mg/kg doses of MEL ($p > 0.05$, Fig. 8 [J]). However, 80 mg/kg dose of MEL significantly increased the concentration of p-CREB compared to the GWI-Veh group ($p < 0.001$, Fig. 8 [J]). Thus, chronic GWI is associated with a significant down-regulation of the BDNF-ERK-CREB signaling pathway. MEL treatment, particularly at 40–80 mg/kg doses, activated this signaling pathway.

3.14. MEL reduced synapse loss in the hippocampus of GWI rats

We investigated whether MEL treatment at 80 mg/kg resulted in reduced synapse loss in the hippocampus of GWI rats. Examples of Syn+ and PSD95+ puncta in the dentate ML of rats belonging to naïve, GWI-Veh, and GWI-MEL80 groups are illustrated (Fig. 8 [K–S]). Area fraction analysis using Image J demonstrated differences between groups for both Syn+ and PSD95+ puncta in the dentate ML and the CA1 subfield ($p < 0.01$, $F = 7.9$ – 11.8 , Fig. 8 [T–W]). Post-hoc analysis revealed reduced Syn+ and PSD95+ puncta in both dentate ML and the CA1 subfield of the GWI-Veh group compared to the naïve control group ($p < 0.05$ – 0.01 , Fig. 8 [T–W]). Furthermore, area fractions of Syn+ and PSD95+ puncta in both regions were higher in the GWI-MEL80 group than the GWI-Veh group ($p < 0.01$, Fig. 8 [T–W]) and comparable to the naïve control group ($p > 0.05$, Fig. 8 [T–W]). The results imply that MEL treatment at 80 mg/kg restrained the loss of synapses in the hippocampus of rats with chronic GWI.

4. Discussion

This study demonstrated the efficacy of low to moderate MEL doses for improving cognitive and mood function in a rat model of chronic GWI. Cognitive and mood impairments are the significant CNS-related symptoms in veterans with GWI [4–6,46,47]. The presence of hippocampus dysfunction could be seen from magnetic resonance spectroscopy and single-photon emission computed tomography studies [48–51] and arterial spin labeling with hippocampal function assessment [52]. Studies using a face-name associative recall test with functional MRI also revealed memory impairment in GWI [3,47]. Furthermore, a meta-analysis has revealed impaired visuospatial, attention, executive, learning, and memory functions in veterans with GWI [5]. Regarding mood function, a study has suggested that the severity of mood dysfunction in GWI varies in its extent but leads to mental health illness at the higher end [53]. Studies have suggested that chronic activation of the executive control network [54,55] and functional connectivity

impairments [56] are the likely causes of cognitive fatigue or dysfunction in GWI. The role of altered cerebral blood flow [57], neuroinflammation [26], and atrophy of brain regions [58,59] have also been suggested as potential causes of Impaired cognitive and mood impairments in veterans with GWI. The perpetuation of neurodegenerative processes and reactive glial changes in veterans with GWI could also be inferred from raised autoantibodies against neuron- and glia-specific proteins in the blood [60].

Several animal models of GWI have replicated cognitive and mood impairments and neuropathology observed in veterans with GWI [16–22,61]. Importantly, analyses of brain tissues at multiple time-points after exposure to GWI-related chemicals revealed the continuation of elevated oxidative stress and significant neuroinflammation [16,21–25,62]. The current study also demonstrated that cognitive and mood dysfunction in rats with chronic GWI (i.e., the GWI-Veh group) is associated with elevated levels of oxidative stress and chronic inflammation in the hippocampus at ~10 months after exposure to GWI-related chemicals and stress. Increased oxidative stress was evident from the higher concentration of lipid peroxidation marker MDA and the protein oxidation marker PCs. Moreover, the concentration of NRF-2, the master regulator of oxidative stress and antioxidant activity, was reduced. Besides, reduced catalase and mitochondrial complexes I–IV confirmed persistent oxidative stress conditions impacting mitochondrial function in the hippocampus. Elevated oxidative stress associated with mitochondrial dysfunction could impact cognitive function [63,64]. Cognitive and mood function can also be affected directly by neuroinflammation or indirectly through its effects on hippocampal neurogenesis [65,66], as neurogenesis contributes to the maintenance of better cognitive and mood function [67–69]. In this study, chronic neuroinflammation in GWI rats could be gleaned from significant astrocyte hypertrophy, a higher number of activated microglia with NLRP3 inflammasomes, increased NF- κ B signaling, elevated levels of proinflammatory cytokines IL-18, TNF- α , IFN- γ , MCP-1, and MIP-1 α . The hippocampus in rats with chronic GWI also displayed significantly reduced neurogenesis, synapse loss, and dampened BDNF-ERK-CREB signaling. Thus, studies in veterans with GWI and animal prototypes of GWI imply that multiple factors, including incessant oxidative stress, neuroinflammation, and alterations in signaling pathways mediating pro-cognitive effects underlie cognitive and mood dysfunction in GWI. Such a conclusion is supported by findings that incessant oxidative stress and neuroinflammation could induce cognitive problems and depression [70–72].

From the above perspectives, compounds with robust antioxidant, antiinflammatory, and pro-cognitive effects have received attention, some of which are currently the focus of several clinical trials in veterans with chronic GWI [6]. Our results provide evidence in support of employing low to moderate doses of MEL for improving cognitive and mood function in chronic GWI. While improvements in simple cognitive tasks such as the novel object recognition and associative recognition memory could be accomplished with both low and moderate doses of MEL (10–80 mg/kg), improvement in a more complex cognitive task such as the hippocampus-dependent object location memory appeared to require a relatively higher dose (80 mg/kg) of MEL. However, anhedonia in GWI rats could be reversed with all MEL doses tested in the study. Characterization of cellular and molecular changes in the hippocampus suggested that MEL's antioxidant, antiinflammatory, and pro-cognitive effects underlie improved cognitive and mood function in GWI rats. Specifically, MEL treatment at 10 mg/kg curtailed oxidative stress markers MDA and PCs, enhanced the antioxidant glutathione and mitochondrial complex III, and diminished the percentage of microglia with NLRP3 inflammasomes, and the concentration of IL-18, TNF- α , and IFN- γ . MEL at 20 mg/kg also normalized the concentration of NRF-2, and catalase, and ramification of microglia whereas, MEL at 40 mg/kg, in addition, lessened astrocyte hypertrophy, the percentage of activated microglia, modulated NF- κ B-NLRP3-caspase-1 signaling, and diminished the concentration of IL-1 β , MCP-1, and MIP-1 α .

Furthermore, MEL at 80 mg/kg enhanced neurogenesis, reduced synapse loss, and activated the BDNF-ERK-CREB signaling pathway.

The current study provides evidence for MEL's competence to mediate robust antioxidant and antiinflammatory effects in a model of chronic GWI. Inflammation typically results in oxidative stress, and oxidative stress can also induce inflammatory responses when caused by mitochondrial dysfunction [73]. MEL is a broad-spectrum antioxidant that can mediate its effects by both direct scavenging or indirect detoxification of ROS, which may comprise enhanced NRF2 and antioxidant levels, mitochondrial protection, reduced ROS formation by inhibiting electron leakage, and suppression of neuronal hyperexcitability [35,73,74]. In the current study, different doses of MEL reduced oxidative stress with the upregulation of glutathione alone (10 mg/kg), and glutathione, catalase, and NRF2 (20–80 mg/kg). All of these effects, in turn, could reduce the extent of inflammation or counteract the consequences of inflammation by reducing ROS levels [75]. MEL treatment also enhanced mitochondrial complex proteins in the hippocampus of GWI rats, with 10–40 mg/kg doses normalizing the complex III protein and 80 mg/kg dose normalizing complexes I, II, and III to levels seen in the hippocampus of naïve control rats.

MEL therapy in this study also mediated direct antiinflammatory effects by inhibiting the formation of NLRP3 inflammasomes [38]. NLRP3 inflammasomes, multiprotein complexes in the cytosol produced by danger-associated molecular patterns (DAMPs) in the CNS, activate the proinflammatory caspase-1, evolves the proinflammatory state, and release mature IL-1 β and IL-18 [76]. In illnesses that display incessantly elevated ROS, such as in GWI, heme, and metabolites could also serve as DAMPs [77]. The configuration of the NLRP3 inflammasome in sequence encompasses NF- κ B activation via DAMPs, the rise of NLRP3 and pro-IL-1 β by NF- κ B [76], and ultimately the NLRP3 inflammasome activation [76]. The NLRP3 inflammasome components include NLR, ASC, and procaspase-1, with ASC serving as a connector that associates NLR with the procaspase-1 [76,77]. The continuous fabrication of NLRP3 inflammasomes in the hippocampus of rats with chronic GWI in this study could be gleaned from elevated levels of NF- κ B, NLRP3, caspase-1, and IL-18. Also, augmented inflammasomes could be seen from NLRP3-ASC complexes in the cytosol of microglia and neurons. MEL therapy reduced the number of inflammasomes per unit area, percentages of microglia with inflammasomes, and the concentration of IL-18 at 10–80 mg/kg dose. At 20–80 mg/kg doses, MEL reduced the concentration of NLRP3, and at 40–80 mg/kg doses, MEL reduced the concentration of NF- κ B, caspase-1, and IL-1 β , implying that MEL treatment decreased inflammasome formation through modulation of NF- κ B signaling in a dose-dependent manner. The ability of MEL to inhibit inflammasome formation via NF- κ B modulation has been seen in several other conditions [39,40,78–80]. Furthermore, reduced concentration of TNF- α , IFN- γ , MCP-1, and MIP-1 α , and lessened astrocyte hypertrophy and activated microglia seen in GWI rats receiving MEL are likely the downstream effects of NF- κ B modulation and NLRP3 inflammasome inhibition [81,82]. MEL can also directly reduce inflammation, which was evident in a previous study from rises in proinflammatory cytokines in aged rats subjected to constant light (a MEL reducing approach) and reversal of such effects with subsequent MEL treatment [83]. Studies have also shown that MEL can suppress proinflammatory cytokines through TLR4 inhibition [84]. Thus, MEL-mediated improved brain function in this study appeared to be due to antioxidant effects at lower doses (10–20 mg/kg) and both antioxidant and robust antiinflammatory effects at moderate doses of MEL (40–80 mg). Furthermore, the reduced hippocampal neurogenesis observed in GWI rats improved with 80 mg/kg MEL but not with lower MEL doses. Such an effect may suggest that relatively higher MEL doses indirectly improve neurogenesis through its robust antioxidant and antiinflammatory effects in neurogenic niches. This finding is concordant with the earlier observations that neurogenesis is sensitive to ROS levels and inflammatory microenvironment [22,85].

Cognitive impairment could also occur through alterations in the

BDNF-ERK-CREB pathway. BDNF, vital for neuronal survival and synaptic plasticity [86], binds to tropomyosin receptor kinase B (TrkB) to promote the activation of several intracellular signaling cascades, including the MAPK/ERK pathway [87]. Through its downstream signaling molecules, pERK promotes the phosphorylation of the transcription factor CREB resulting in BDNF transcription through binding of pCREB to the BDNF promoter region [88]. The BDNF-ERK-CREB pathway is critical for sustaining neuronal survival, synapses, and synaptic plasticity [89]. Furthermore, reduced concentration of BDNF in the brain is one of the features of cognitive dysfunction in many brain disorders [90,91]. This study showed that cognitive dysfunction in rats with chronic GWI was associated with diminished BDNF-ERK-CREB signaling in the hippocampus, and 80 mg/kg MEL therapy activated this signaling to levels seen in naïve control rats. It has been shown earlier that MEL activates the BDNF-ERK-CREB signaling pathway through its action on MEL receptor 1 [37]. Activation of BDNF-ERK-CREB signaling with 80 mg/kg MEL also correlated with improved hippocampal neurogenesis, reduced synapse loss, and better ability for the most complex hippocampus-dependent cognitive task (i.e., the object location memory) assessed in the study. These findings match the earlier observations that MEL can improve neurogenesis through modulation of neurogenesis regulators such as BDNF and p-CREB [92] and that the memory formation and storage in the hippocampus requires activation of the ERK pathway and CREB phosphorylation [93,94].

5. Conclusions

The study demonstrated that MEL therapy is efficacious for improving cognitive and mood function in a rat model of chronic GWI. However, MEL's effect was dose-dependent, with lower (10–20 mg/kg) doses improving simple and associative recognition memory function in association with reductions in oxidative stress and some neuroinflammatory markers. Moderate MEL doses (40–80 mg/kg), in addition to antioxidant effects, mediated robust antiinflammatory activity through inhibition of NLRP3 inflammasomes. MEL at 80 mg/kg also activated the BDNF-ERK-CREB signaling pathway, enhanced neurogenesis and reduced synapse loss in the hippocampus, and improved a more complex hippocampus-dependent cognitive function. Overall, the study provides the first evidence of MEL's promise for alleviating neuroinflammation and cognitive and mood impairments in veterans afflicted with GWI.

Department of defense, United States government disclaimer

The contents of this article suggest the views of authors and do not represent the views of the Department of Defense or the United States Government.

Author contribution

Concept: AKS. Research design: AKS, LNM, MK, and SA. Data collection, analysis and interpretation: LNM, MK, SA, BS, LM, XR, and AKS. Preparation of figure composites: LNM, MK, SA, and AKS. Manuscript writing: LNM and AKS. All authors provided feedback and edits to the manuscript text and approved the final version of the manuscript.

Declaration of competing interest

The authors declared no conflicts of interest.

Acknowledgments

This work was mainly supported by grants from the Department of Defense (GWIRP grants, W81XWH-17-1-0447 and W81XWH-16-1-0480 to AKS) and partly by the National Institutes of Health Grant

(R01NS106907-01 to AKS).

References

- [1] B.A. Golomb, Acetylcholinesterase inhibitors and Gulf war illnesses, *Proc. Natl. Acad. Sci. U. S. A.* 105 (11) (2008) 4295–4300.
- [2] Institute of Medicine, *Chronic Multisymptom Illness in Gulf War Veterans: Case Definitions Reexamined*, The National Academies Press, Washington, DC, 2014.
- [3] T.N. Odegard, C.M. Cooper, E.A. Farris, J. Arduengo, J. Bartlett, R. Haley, Memory impairment exhibited by veterans with Gulf war illness, *Neurocase* 19 (4) (2013) 316–327.
- [4] R.F. White, L. Steele, J.P. O'Callaghan, et al., Recent research on Gulf War illness and other health problems in veterans of the 1991 Gulf War: effects of toxicant exposures during deployment, *Cortex* 74 (2016) 449–475.
- [5] P.A. Janulewicz, M.H. Krengel, A. Maule, et al., Neuropsychological characteristics of Gulf War illness: a meta-analysis, *PLoS One* 12 (5) (2017), e0177121.
- [6] B. Dickey, L.N. Madhu, A.K. Shetty, Gulf war illness: mechanisms underlying brain dysfunction and promising therapeutic strategies, *Pharmacol. Ther.* 220 (2021) 107716.
- [7] R.W. Haley, T.L. Kurt, Self-reported exposure to neurotoxic chemical combinations in the Gulf War. A cross-sectional epidemiologic study, *J. Am. Med. Assoc.* 277 (3) (1997) 231–237.
- [8] L. Steele, Prevalence and patterns of Gulf War illness in Kansas veterans: association of symptoms with characteristics of person, place, and time of military service, *Am. J. Epidemiol.* 152 (10) (2000) 992–1002.
- [9] J.H. Binns, C. Barlow, F.E. Bloom, et al., Gulf War Illness and the Health of Gulf War Veterans: Scientific Findings and Recommendations, Research Advisory Committee Report on Gulf War Illness and Health of Gulf War Veterans, Dept of Veterans Affairs. US Government Printing Office, Washington, DC, 2008, pp. 1–465.
- [10] National Academies of Sciences, Engineering, and medicine, in: *Gulf War and Health*, volume 11, Generational Health Effects of Serving in the Gulf War, Washington (DC), 2018.
- [11] G. Bjorklund, L. Pivina, M. Dadar, et al., Depleted uranium and Gulf War Illness: updates and comments on possible mechanisms behind the syndrome, *Environ. Res.* 181 (2020) 108927.
- [12] A. Abdel-Rahman, A.K. Shetty, M.B. Abou-Donia, Subchronic dermal application of N,N-diethyl m-toluamide (DEET) and permethrin to adult rats, alone or in combination, causes diffuse neuronal cell death and cytoskeletal abnormalities in the cerebral cortex and the hippocampus, and Purkinje neuron loss in the cerebellum, *Exp. Neurol.* 172 (1) (2001) 153–171.
- [13] A. Abdel-Rahman, A.K. Shetty, M.B. Abou-Donia, Disruption of the blood-brain barrier and neuronal cell death in cingulate cortex, dentate gyrus, thalamus, and hypothalamus in a rat model of Gulf-War syndrome, *Neurobiol. Dis.* 10 (3) (2002) 306–326.
- [14] A. Abdel-Rahman, A.K. Shetty, M.B. Abou-Donia, Acute exposure to sarin increases blood brain barrier permeability and induces neuropathological changes in the rat brain: dose-response relationships, *Neuroscience* 113 (3) (2002) 721–741.
- [15] L. Abdullah, G. Crynen, J. Reed, et al., Proteomic CNS profile of delayed cognitive impairment in mice exposed to Gulf War agents, *NeuroMolecular Med.* 13 (4) (2011) 275–288.
- [16] V.K. Parihar, B. Hattiangady, B. Shuai, A.K. Shetty, Mood and memory deficits in a model of Gulf War illness are linked with reduced neurogenesis, partial neuron loss, and mild inflammation in the hippocampus, *Neuropsychopharmacology* 38 (12) (2013) 2348–2362.
- [17] B. Hattiangady, V. Mishra, M. Kodali, B. Shuai, X. Rao, A.K. Shetty, Object location and object recognition memory impairments, motivation deficits and depression in a model of Gulf War illness, *Front. Behav. Neurosci.* 8 (2014) 78.
- [18] Z. Zakirova, M. Tweed, G. Crynen, et al., Gulf War agent exposure causes impairment of long-term memory formation and neuropathological changes in a mouse model of Gulf War Illness, *PLoS One* 10 (3) (2015), e0119579.
- [19] K.F. Phillips, L.S. Deshpande, Repeated low-dose organophosphate DFP exposure leads to the development of depression and cognitive impairment in a rat model of Gulf War Illness, *Neurotoxicology* 52 (2016) 127–133.
- [20] M. Kodali, B. Hattiangady, G.A. Shetty, A. Bates, B. Shuai, A.K. Shetty, Curcumin treatment leads to better cognitive and mood function in a model of Gulf War Illness with enhanced neurogenesis, and alleviation of inflammation and mitochondrial dysfunction in the hippocampus, *Brain Behav. Immun.* 69 (2018) 499–514.
- [21] L.N. Madhu, S. Attaluri, M. Kodali, et al., Neuroinflammation in Gulf War Illness is linked with HMGB1 and complement activation, which can be discerned from brain-derived extracellular vesicles in the blood, *Brain Behav. Immun.* 81 (2019) 430–443.
- [22] A.K. Shetty, S. Attaluri, M. Kodali, et al., Monosodium luminol reinstates redox homeostasis, improves cognition, mood and neurogenesis, and alleviates neuro- and systemic inflammation in a model of Gulf War Illness, *Redox Biol* 28 (2020) 101389.
- [23] G.A. Shetty, B. Hattiangady, D. Upadhy, et al., Chronic oxidative stress, mitochondrial dysfunction, Nrf2 activation and inflammation in the Hippocampus accompany heightened systemic inflammation and oxidative stress in an animal model of Gulf war illness, *Front. Mol. Neurosci.* 10 (2017) 182.
- [24] J.P. O'Callaghan, K.A. Kelly, A.R. Locker, D.B. Miller, S.M. Lasley, Corticosterone primes the neuroinflammatory response to DFP in mice: potential animal model of Gulf War Illness, *J. Neurochem.* 133 (5) (2015) 708–721.
- [25] A.R. Locker, L.T. Michalovicz, K.A. Kelly, J.V. Miller, D.B. Miller, J.P. O'Callaghan, Corticosterone primes the neuroinflammatory response to Gulf War Illness-relevant organophosphates independently of acetylcholinesterase inhibition, *J. Neurochem.* 142 (3) (2017) 444–455.
- [26] Z. Alshelhi, D.S. Albrecht, C. Bergan, et al., In-vivo imaging of neuroinflammation in veterans with Gulf War illness, *Brain Behav. Immun.* 87 (2020) 498–507.
- [27] L. Abdullah, J.E. Evans, H. Montague, et al., Chronic elevation of phosphocholine containing lipids in mice exposed to Gulf War agents pyridostigmine bromide and permethrin, *Neurotoxicol. Teratol.* 40 (2013) 74–84.
- [28] L. Abdullah, J.E. Evans, U. Joshi, et al., Translational potential of long-term decreases in mitochondrial lipids in a mouse model of Gulf War Illness, *Toxicology* 372 (2016) 22–33.
- [29] U. Joshi, A. Pearson, J.E. Evans, et al., A permethrin metabolite is associated with adaptive immune responses in Gulf War Illness, *Brain Behav. Immun.* 81 (2019) 545–559. Oct.
- [30] F. Alhasson, S. Das, R. Seth, et al., Altered gut microbiome in a mouse model of Gulf War Illness causes neuroinflammation and intestinal injury via leaky gut and TLR4 activation, *PLoS One* 12 (3) (2017), e0172914.
- [31] R.K. Seth, R. Maqsood, A. Mondal, et al., Gut DNA virome diversity and its association with host bacteria regulate inflammatory phenotype and neuronal immunotoxicity in experimental Gulf war illness, *Viruses* 11 (10) (2019).
- [32] L. Kimono, D. Bose, R.K. Seth, et al., Host akkermansia muciniphila abundance correlates with Gulf war illness symptom persistence via NLRP3-mediated neuroinflammation and decreased brain-derived neurotrophic factor, *Neurosci Insights* 15 (2020), 2633105520942480.
- [33] N. Buscemi, B. Vandermeer, R. Pandya, et al., Melatonin for treatment of sleep disorders, *Evid. Rep. Technol. Assess.* (108) (2004) 1–7.
- [34] M.A. Eghbal, A. Eftekhari, E. Ahmadian, Y. Azarni, A. Parvizpur, A review of biological and pharmacological actions of melatonin: oxidant and prooxidant properties, *Pharm. Bioprocess.* 4 (4) (2016), 069–081.
- [35] R.J. Reiter, J.C. Mayo, D.X. Tan, R.M. Sainz, M. Alatorre-Jimenez, L. Qin, Melatonin as an antioxidant: under promises but over delivers, *J. Pineal Res.* 61 (3) (2016) 253–278.
- [36] K. Ding, H. Wang, J. Xu, X. Lu, L. Zhang, L. Zhu, Melatonin reduced microglial activation and alleviated neuroinflammation induced neuron degeneration in experimental traumatic brain injury: possible involvement of mTOR pathway, *Neurochem. Int.* 76 (2014) 23–31.
- [37] J.Y. Sung, J.H. Bae, J.H. Lee, Y.N. Kim, D.K. Kim, The melatonin signaling pathway in a long-term memory in vitro study, *Molecules* 23 (4) (2018).
- [38] G. Favero, L. Franceschetti, F. Bonomini, L.F. Rodella, R. Rezzani, Melatonin as an anti-inflammatory agent modulating inflammasome activation, *Internet J. Endocrinol.* 2017 (2017) 1835195.
- [39] I. Rahim, B. Djerdjouri, R.K. Sayed, et al., Melatonin administration to wild-type mice and nontreated NLRP3 mutant mice share similar inhibition of the inflammatory response during sepsis, *J. Pineal Res.* 63 (1) (2017).
- [40] H. Volt, J.A. Garcia, C. Doerrier, et al., Same molecule but different expression: aging and sepsis trigger NLRP3 inflammasome activation, a target of melatonin, *J. Pineal Res.* 60 (2) (2016) 193–205.
- [41] G.R. Barker, E.C. Warburton, Object-in-place associative recognition memory depends on glutamate receptor neurotransmission within two defined hippocampal-cortical circuits: a critical role for AMPA and NMDA receptors in the hippocampus, perirhinal, and prefrontal cortices, *Cerebr. Cortex* 25 (2) (2015) 472–481.
- [42] D. Upadhy, B. Hattiangady, G.A. Shetty, G. Zanirati, M. Kodali, A.K. Shetty, Neural stem cell or human induced pluripotent stem cell-derived GABA-ergic progenitor cell grafting in an animal model of chronic temporal lobe epilepsy, *Curr Protoc Stem Cell Biol* 38 (2016), 2D 7 1-2D 7 47.
- [43] M.S. Rao, B. Hattiangady, A.K. Shetty, Status epilepticus during old age is not associated with enhanced hippocampal neurogenesis, *Hippocampus* 18 (9) (2008) 931–944.
- [44] B. Hattiangady, R. Kuruba, A.K. Shetty, Acute seizures in old age leads to a greater loss of CA1 pyramidal neurons, an increased propensity for developing chronic TLE and a severe cognitive dysfunction, *Aging Dis* 2 (2011) 1–17, 1.
- [45] M. Kodali, T. Megahed, V. Mishra, B. Shuai, B. Hattiangady, A.K. Shetty, Voluntary running exercise-mediated enhanced neurogenesis does not obliterate retrograde spatial memory, *J. Neurosci.* 36 (31) (2016) 8112–8122.
- [46] B.N. Smith, J.M. Wang, D. Vogt, K. Vickers, D.W. King, L.A. King, Gulf war illness: symptomatology among veterans 10 years after deployment, *J. Occup. Environ. Med.* 55 (1) (2013) 104–110.
- [47] C.M. Cooper, R.W. Briggs, E.A. Farris, J. Bartlett, R.W. Haley, T.N. Odegard, Memory and functional brain differences in a national sample of U.S. veterans with Gulf War Illness, *Psychiatry Res. Neuroimaging.* 250 (2016) 33–41.
- [48] R.W. Haley, J.L. Fleckenstein, W.W. Marshall, G.G. McDonald, G.L. Kramer, F. Petty, Effect of basal ganglia injury on central dopamine activity in Gulf War syndrome: correlation of proton magnetic resonance spectroscopy and plasma homovanillic acid levels, *Arch. Neurol.* 57 (9) (2000) 1280–1285.
- [49] R.W. Haley, W.W. Marshall, G.G. McDonald, M.A. Daugherty, F. Petty, J. L. Fleckenstein, Brain abnormalities in Gulf War syndrome: evaluation with 1H MR spectroscopy, *Radiology* 215 (3) (2000) 807–817.
- [50] R.W. Haley, J.S. Spence, P.S. Carmack, et al., Abnormal brain response to cholinergic challenge in chronic encephalopathy from the 1991 Gulf War, *Psychiatr. Res.* 171 (3) (2009) 207–220.
- [51] P.M. Menon, H.A. Nasrallah, R.R. Reeves, J.A. Ali, Hippocampal dysfunction in Gulf War Syndrome. A proton MR spectroscopy study, *Brain Res.* 1009 (1–2) (2004) 189–194.

- [52] X. Li, J.S. Spence, D.M. Buhner, et al., Hippocampal dysfunction in Gulf War veterans: investigation with ASL perfusion MR imaging and physostigmine challenge, *Radiology* 261 (1) (2011) 218–225.
- [53] B.E. Engdahl, L.M. James, R.D. Miller, et al., Brain function in Gulf war illness (GWI) and associated mental health comorbidities, *J Neurol Neuromedicine* 3 (4) (2018) 24–34.
- [54] M. D'Esposito, B.R. Postle, The cognitive neuroscience of working memory, *Annu. Rev. Psychol.* 66 (2015) 115–142.
- [55] G.R. Wylie, H. Genova, E. Dobryakova, et al., Fatigue in Gulf War Illness is associated with tonically high activation in the executive control network, *Neuroimage Clin* 21 (2019) 101641.
- [56] K.S. Gopinath, U. Sakoglu, B.A. Crosson, R.W. Haley, Exploring brain mechanisms underlying Gulf War Illness with group ICA based analysis of fMRI resting state networks, *Neurosci. Lett.* 701 (2019) 136–141.
- [57] M.J. Falvo, J.B. Lindheimer, J.M. Serrador, Dynamic cerebral autoregulation is impaired in Veterans with Gulf War Illness: a case-control study, *PLoS One* 13 (10) (2018), e0205393.
- [58] P. Christova, L.M. James, B.E. Engdahl, S.M. Lewis, A.F. Carpenter, A. P. Georgopoulos, Subcortical brain atrophy in Gulf war illness, *Exp. Brain Res.* 235 (9) (2017) 2777–2786.
- [59] Y. Zhang, T. Avery, A.A. Vakhtin, et al., Brainstem atrophy in Gulf war illness, *Neurotoxicology* 78 (2020) 71–79.
- [60] M.B. Abou-Donia, L.A. Conboy, E. Kokkotou, et al., Screening for novel central nervous system biomarkers in veterans with Gulf War Illness, *Neurotoxicol. Teratol.* 61 (2017) 36–46.
- [61] K.F. Phillips, E. Santos, R.E. Blair, L.S. Deshpande, Targeting intracellular calcium stores alleviates neurological morbidities in a DFP-based rat model of Gulf war illness, *Toxicol. Sci.* 169 (2) (2019) 567–578.
- [62] Z. Zakirova, G. Crynen, S. Hassan, et al., A chronic longitudinal characterization of neurobehavioral and neuropathological cognitive impairment in a mouse model of Gulf war agent exposure, *Front. Integr. Neurosci.* 9 (2016) 71.
- [63] M.B. Netto, A.N. de Oliveira Junior, M. Goldim, et al., Oxidative stress and mitochondrial dysfunction contributes to postoperative cognitive dysfunction in elderly rats, *Brain Behav. Immun.* 73 (2018) 661–669.
- [64] A. Fernandez, D.W. Meechan, B.A. Karpinski, et al., Mitochondrial dysfunction leads to cortical under-connectivity and cognitive impairment, *Neuron* 102 (6) (2019) 1127–1142, e1123.
- [65] B. Kaltschmidt, C. Kaltschmidt, NF-KappaB in long-term memory and structural plasticity in the adult mammalian brain, *Front. Mol. Neurosci.* 8 (2015) 69.
- [66] K.M. McAvoy, A. Sahay, Targeting adult neurogenesis to optimize hippocampal circuits in aging, *Neurotherapeutics* 14 (3) (2017) 630–645.
- [67] L. Santarelli, M. Saxe, C. Gross, et al., Requirement of hippocampal neurogenesis for the behavioral effects of antidepressants, *Science* 301 (5634) (2003) 805–809.
- [68] W. Deng, J.B. Aimone, F.H. Gage, New neurons and new memories: how does adult hippocampal neurogenesis affect learning and memory? *Nat. Rev. Neurosci.* 11 (5) (2010) 339–350.
- [69] J.S. Snyder, A. Soumier, M. Brewer, J. Pickel, H.A. Cameron, Adult hippocampal neurogenesis buffers stress responses and depressive behaviour, *Nature* 476 (7361) (2011) 458–461.
- [70] R. Krishnadas, J. Cavanagh, Depression: an inflammatory illness? *J. Neurol. Neurosurg. Psychiatry* 83 (5) (2012) 495–502.
- [71] S. Navakkode, C. Liu, T.W. Soong, Altered function of neuronal L-type calcium channels in ageing and neuroinflammation: implications in age-related synaptic dysfunction and cognitive decline, *Ageing Res. Rev.* 42 (2018) 86–99.
- [72] A.S. Carlessi, L.A. Borba, A.I. Zugno, J. Quevedo, G.Z. Reus, Gut microbiota-brain axis in depression: the role of neuroinflammation, *Eur. J. Neurosci.* 53 (1) (2021) 222–235.
- [73] R. Hardeland, Melatonin and inflammation—Story of a double-edged blade, *J. Pineal Res.* 65 (4) (2018), e12525.
- [74] R. Hardeland, D.P. Cardinali, G.M. Brown, S.R. Pandi-Perumal, Melatonin and brain inflammaging, *Prog. Neurobiol.* 127–128 (2015) 46–63.
- [75] I.A. Ismail, H.A. El-Bakry, S.S. Soliman, Melatonin and turmeric ameliorate aging-induced changes: implication of immunoglobulins, cytokines, DJ-1/NRF2 and apoptosis regulation, *Int J Physiol Pathophysiol Pharmacol* 10 (2) (2018) 70–82.
- [76] S. Voet, S. Srinivasan, M. Lamkanfi, G. van Loo, Inflammasomes in neuroinflammatory and neurodegenerative diseases, *EMBO Mol. Med.* 11 (6) (2019) e10248.
- [77] M. Lamkanfi, V.M. Dixit, Inflammasomes and their roles in health and disease, *Annu. Rev. Cell Dev. Biol.* 28 (2012) 137–161.
- [78] F. Ortiz, D. Acuna-Castroviejo, C. Doerrier, et al., Melatonin blunts the mitochondrial/NLRP3 connection and protects against radiation-induced oral mucositis, *J. Pineal Res.* 58 (1) (2015) 34–49.
- [79] Y. Dong, C. Fan, W. Hu, et al., Melatonin attenuates early brain injury induced by subarachnoid hemorrhage via regulating NLRP3 inflammasome and apoptosis signaling, *J. Pineal Res.* 60 (3) (2016) 253–262.
- [80] Z. Cao, Y. Fang, Y. Lu, et al., Melatonin alleviates cadmium-induced liver injury by inhibiting the TXNIP-NLRP3 inflammasome, *J. Pineal Res.* 62 (3) (2017).
- [81] T. Lawrence, The nuclear factor NF-kappaB pathway in inflammation, *Cold Spring Harb Perspect Biol* 1 (6) (2009), a001651.
- [82] R. Saggü, T. Schumacher, F. Gerich, et al., Astroglial NF-kB contributes to white matter damage and cognitive impairment in a mouse model of vascular dementia, *Acta Neuropathol Commun* 4 (1) (2016) 76.
- [83] H.A. El-Bakry, I.A. Ismail, S.S. Soliman, Immunosenescence-like state is accelerated by constant light exposure and counteracted by melatonin or turmeric administration through DJ-1/Nrf2 and P53/Bax pathways, *J. Photochem. Photobiol., B* 186 (2018) 69–80.
- [84] M.Z. Xia, Y.L. Liang, H. Wang, et al., Melatonin modulates TLR4-mediated inflammatory genes through MyD88- and TRIF-dependent signaling pathways in lipopolysaccharide-stimulated RAW264.7 cells, *J. Pineal Res.* 53 (4) (2012) 325–334.
- [85] T.T. Huang, D. Leu, Y. Zou, Oxidative stress and redox regulation on hippocampal-dependent cognitive functions, *Arch. Biochem. Biophys.* 576 (2015) 2–7.
- [86] P. Kowiański, G. Lietzau, E. Czuba, M. Waskow, A. Steliga, J. Moryś, BDNF: a key factor with multipotent impact on brain signaling and synaptic plasticity, *Cell. Mol. Neurobiol.* 38 (3) (2018) 579–593.
- [87] L. Minichiello, TrkB signalling pathways in LTP and learning, *Nat. Rev. Neurosci.* 10 (12) (2009) 850–860.
- [88] L.F. Reichardt, Neurotrophin-regulated signalling pathways, *Philos. Trans. R. Soc. Lond. B Biol. Sci.* 361 (1473) (2006) 1545–1564.
- [89] S. Finkbeiner, S.F. Tavazoie, A. Maloratsky, K.M. Jacobs, K.M. Harris, M. E. Greenberg, CREB: a major mediator of neuronal neurotrophin responses, *Neuron* 19 (5) (1997) 1031–1047.
- [90] S.A. Heldt, L. Stanek, J.P. Chhatwal, K.J. Ressler, Hippocampus-specific deletion of BDNF in adult mice impairs spatial memory and extinction of aversive memories, *Mol. Psychiatr.* 12 (7) (2007) 656–670.
- [91] C.A. Saura, J. Valero, The role of CREB signaling in Alzheimer's disease and other cognitive disorders, *Rev. Neurosci.* 22 (2) (2011) 153–169.
- [92] J.W. Leung, K.K. Cheung, S.P. Ngai, H.W. Tsang, B.W. Lau, Protective effects of melatonin on neurogenesis impairment in neurological disorders and its relevant molecular mechanisms, *Int. J. Mol. Sci.* 21 (16) (2020) 5645.
- [93] C. O'Connell, H.C. Gallagher, A. O'Malley, M. Bourke, C.M. Regan, CREB phosphorylation coincides with transient synapse formation in the rat hippocampal dentate gyrus following avoidance learning, *Neural Plast.* 7 (4) (2000) 279–289.
- [94] M.G. Giovannini, The role of the extracellular signal-regulated kinase pathway in memory encoding, *Rev. Neurosci.* 17 (6) (2006) 619–634.